A study of live neural cell in cultured neural network by using Raman spectroscopy

A Thesis for the Degree

of

Doctor of Science

A study of live neural cell in cultured neural network by using Raman spectroscopy

Submitted to

Department of Bioscience,

Graduate School of Science & Technology,

Kwansei Gakuin University

By

Kosuke Hashimoto

March, 2019

Abstract

Neural cells were studied using Raman spectroscopy. During development, a stem cell produces a neural progenitor that is able to propagate itself. However, once the neural progenitor cell differentiates into a neural cell, the cell cycle arrests at G_0, and the cell does not propagate anymore, but it matures. Raman spectroscopy has been applied for analysis of various cells, but very few studies have used it for analysis of neural cells. The purpose of the present study was to study the function of an intact brain using an optical technology. In the present study, I used label-free techniques to analyze live neural cells by Raman spectroscopy and demonstrated its potential in the analysis of live neural cells. An analytical model of a maturing neural cell has been developed, which showed that the process of maturation is not linear, but divided into stages that correlate with its electrical signaling functions. There are two types of neural cells, excitatory and inhibitory. It is very difficult to distinguish between these two types solely based on morphological evidence without staining. Raman analysis is able to discriminate between these two types of cells in a totally noninvasive manner. This technique has been applied to analyze the effects of bisphenol A (BPA). It was known that BPA inhibits the spontaneous signaling function of neural cells in vitro. The results suggested that BPA does not prevent maturation of the cell, but it interferes with specific signaling molecules present within the cell. The results of the present work strongly demonstrate that Raman analysis is a highly powerful tool for studying intact neural cells.

Contents

General introduction

The final goal of the present study is to investigate the process through which neural cells mature and gain their function in a developing intact brain. The knowledge and technology resulting from this research will contribute greatly to the field of higher brain functions. Exploration of the molecular mechanisms of neural maturation during fetal development and infancy may lead to an understanding of the development of mental activity, and may contribute to the identification of therapies and preventative measures for diseases of the central nervous system, such as Alzheimer-type dementia and Parkinson's disease. Brain function has been studied at various levels of the functional unit. In broader terms, the functions of the brain may be categorized into two concepts; a physical and physiological function, and a conscious and emotional function. These two functions are closely related to each other. The former controls body parts that physically exist, which are classified into lower functional concepts such as motility, physiology, homeostasis, and so on. Parkinson's disease destroys dopaminergic neurons and degenerates the physical function of the brain.[1] The latter is a source of intellect that is free from any physical restriction and is predominantly controlled by the cerebral cortex. Alzheimer's disease is attributed to accumulation of β-amyloid in the extracellular domains of the brain, thus leading to dystrophy of neurons and atrophy of the hippocampus.[2] It has been suggested that a specific area on the brain surface may have a connection to functions of specific body parts. This is referred to as the theory of localization of brain function, according to which the brain is built of many small components.

The brain generally has a layered structure. For example, the cerebral cortex consists of 6 layers; a molecular layer, an external granule cell layer, an external pyramidal cell layer, an internal granule cell layer, an internal pyramidal cell layer, and a multiform layer.[3] Each layer has a different composition of neural and other cells. The cells that propagates the signal are, however, only the neural cells.

Although there are various types of cells in the brain, brain function is the result of electric signal processing in the neural network built by neural cells. Neural cells play the role of the electric wires, condensers, transistors, distributors, and so on, to organize a huge circuit to process input signals. When we regard brain function as information processing between input and output, the whole processing consists of small units of signal processing held in the smallest unit device, the neural cell, like a computer. Hopfield and Tank developed a new conceptual framework mimicking neural circuits to study the signal process in the brain.[4] Their framework consists of artificial neurons arranged in an *n* by *n* array connected with excitatory and inhibitory synapses that are the computational connections. Their model circuit was able to solve difficult problems. In such studies, the character of the neuron is generally uniform, but real neural cells are somewhat different. Boldog et al. found a specialized GABAergic neuron subtype in the human cortex by single-nucleus RNA sequencing.[5] This suggests that there may be different types of neural cells that have not been found yet. I assume that construction of a network system consisting of various neural cells is remarkably important for understanding overall brain functions.

Many methods have already been developed for analyzing brain functions. For example, functional magnetic resonance imaging (fMRI) is one of the most advanced technologies for functional analysis of the whole brain.[6] This method monitors blood flow and oxygenation in the brain, two factors that are deeply related to neural activity.[7] fMRI technology is very useful for studying the mental activity and consciousness in humans because it is a non-invasive method.

Although investigations of the molecular activity of neural cells are also important, it is also necessary to study the fundamental signaling mechanisms of neural cell networks. Currently, there is no non-invasive technology to observe a single cell within a live brain.[8] Since it is impossible to use human patients, the use of animal models is necessary to empirically study neural cells. Electrophysiology is one of the most

effective tools for the functional analysis of the cellular level. It was developed in 18th century. Galvani discovered that when electric stimulation was applied to the nerve in a frog, muscular contractions were observed.[9] Caton reported the experiments in 1875 and noted that an electrical phenomenon was observed in the brains of animals.[10] This discovery was a trigger for the invention of the electroencephalograph (EEG).[11]

Kudoh et al. studied the electric signal generated by neural cells in a cellular network in a culturing dish with multielectrodes. The electrode method is widely used for the study of neural activity in vitro.[12-15] A technique using a membrane potential sensitive dye was developed by Smetters et al. to observe the electrical activity at the single-cell level.[16] They succeeded in the observation of electrophysiological activity using membrane potential sensitive dye imaging (VSDI) in vitro. Live cell observation techniques using dyes and/or gene modification are recognized to be highly effective to study signal transfer and even the electrophysiological activity of a single cell. However, the phenotypic and function effects of such dyes and gene modifications are not well-known. Moreover, these techniques do not give molecular information regarding the functional development in a cell. Consequently, a new technology is needed to observe electrical activity of a live neural cell without any labelling. If it was possible to measure the signaling of the neurons in the intact brain, the study of brain function would proceed drastically.

I am deeply interested in signal processing by neural networks in the brain, especially the 3D physical interactions and electric signal transfers among neurons. This interest motivated me to apply optical techniques to research neural systems. Kawakami et al. succeeded in observing the structure and configuration of neural cells in a live mouse brain with multiphoton fluorescent microscopy.[17] The results clearly indicate that optical techniques are able to access neural cells deep within the brain in a totally noninvasive manner. The fluorescence microscope well depicts the morphology of neural cells in vivo, however, it does not give us any functional information. It is necessary to use another

optical technique to reach this goal. I believe that there must be molecular changes associated with a functional change in a cell. Raman spectroscopy is a technique that may be potentially used to analyze molecular changes in a live cell. During development, an embryonic stem cell differentiates into various types of cells with specific functions. Pascut et al. demonstrated that the differentiation from a human embryonic stem cell into cardiomyocytes was successfully detected by Raman spectroscopy, with multivariate analysis.[18] This study gave me the idea that the function of a cell can be predicted based on its molecular composition and that Raman spectroscopy could be used to determine this composition.

Raman spectroscopy is a vibrational spectroscopy, which differs from infrared (IR) and near-infrared (NIR) spectroscopies. Vibrational spectroscopies provide information by measuring the molecular vibration because each molecule has a specific vibrational pattern consisting of vibrational modes.[19] Therefore, it is able to identify a molecule according to its vibrational spectrum without any labelling. IR and NIR spectroscopies are absorption spectroscopies in which the reduction in light due to absorption of the sample is measured. Since water has strong and broad absorption bands all over the NIR and IR region (1100 nm-25 μm), they are generally applied for dried or semi-dried samples. In contrast, Raman spectroscopy is a scattering spectroscopy. Since any wavelength of light can be utilized for observation, it is relatively easy to avoid the interference of water.

In 1928, C. V. Raman reported the discovery of a new type of scattering light.[20] When a monochroic light is irradiated through a sample, light is scattered by molecules in the sample. While almost scattering light has the same wavelength as the incident light (called Rayleigh scattering), a very weak scattered light with a different wavelength from the incident light is generated. This scattering process is named “Raman scattering” after its discoverer. Rayleigh scattering is attributed to elastic collisions between photons and molecules. Raman scattering takes place as a result of inelastic collisions in which a

photon exchanges its transition energy between vibrational levels with a molecule. The Raman scattered light shifts its wavelength, thus reflecting the molecular vibrational states. Raman spectroscopy has several advantages for biological research compared to conventional molecular biological methods. Raman spectroscopy allows one to make invasion- and contact-free measurements, because the scattered light is observed at any surface, and sub-surface. Since Raman scattered light is generated by all molecules, except some 2 or 3 atoms gas molecules, it is free from labelling. Any monochroic light in the ultraviolet (UV; 190-400 nm), visible (400-800 nm) and near-NIR (800-1100 nm) region is employed for excitation in Raman spectroscopy, which enables to avoid water absorption. There are many more optical instruments available in this spectral region compared to the NIR and IR regions, such as the microscope and optical fibers. A Raman microscope yields spatial resolution as high as a generic light microscope (< 1 μm). A fiber optic Raman probe is able to bring the sampling point inside a live animal or the human body.

In the last decade, remarkable advances in hardware technology such as lasers and detectors and the improvement in computers have allowed us to use Raman spectroscopy easily. Katagiri et al. developed a ball lens installed hollow optical fiber Raman probe (BHRP) [21]and succeeded in acquiring the Raman spectra of live and dead mouse brains.[22] A comparative study suggested that spectral changes may be attributable to compositional changes of the free water clusters in the brain. The results of this study suggested that the structure of the water molecules was related to brain activity. It also demonstrated that Raman spectroscopy has a high potential to analyze molecular dynamics relating to the function of the brain. Oshima et al. demonstrated that several types of human lung cancer cells were successfully identified by Raman microscopy and chemometrics.[23] The data points due to the Raman spectra of single cells were spread over a triaxial coordinate system of a principal composition analysis (PCA) score plot. However, the datasets in the same cell group were successfully categorized into

characteristic groups according to their types. There are more than 10,000 different molecules in a live cell and its Raman spectrum consists of spectra of all the materials existing in the cell. A live cell always changes its molecular composition because of the cell cycle and its physiological reactions. The characteristic dynamism of living things is referred to as homeostasis. Consequently, chemometric techniques have been applied in the present study to recognize the molecular changes due to cellular reactions due to normal homeostasis. Torimitsu et al. successfully detected the release of glutamate in synaptosomes by Raman spectroscopy using laser trapping. They suggested that Raman spectroscopy has a high potential for monitoring the functional molecular changes at molecular sizes that are too small to be labeled.[24]

The present study provides fundamental knowledge to identify the relationship between the function and molecular characteristics of a neural cell. I used a primary culture of neural cells obtained from a rat fetus as a neural developmental model. Neurons in a cell culture dish spontaneously develop spontaneously a network structure that is a very simple model of the neural network in the brain. From a morphological point of view, the development of neurons is schematically described by the progression of neurites, acquiring polarity and forming the spine.[25, 26] These cellular reactions are considered to be the growth process of the neural network. From the viewpoint of electrophysiology, a neuron generates electrical signals such as spontaneous firing at an early stage and synchronized firing later.[12, 13]

In chapter 1, I studied the molecular changes taking place in growing neural cells in vitro using Raman spectroscopy. Cellular maturation is a characteristic phenomenon only of neural cells because other cells are usually regenerating during the cell cycle. These results suggest that the maturation of a neural cell consists of several stages correlated with their functional development and the maturation stage is estimated by its molecular composition analyzed by Raman spectroscopy.

In chapter 2, I succeeded in discriminating between excitatory and inhibitory

neural cells in a totally noninvasive manner. It was quite difficult to observe the polarity of live neural cells because a conventional method such as immune-staining was used. A discrimination model has been developed for intact neural cells based on Raman analysis and its reliability is evaluated using totally independent test datasets.

In chapter 3, I studied the effects of an endocrine disruptor, bisphenol A (BPA), in growing neural cells. The results suggest that BPA does not inhibit nor accelerate cellular growth but causes changes in the molecular compositional of the exposed cell.

References

1. W. Dauer and S. Przedborski, *Neuron*, 2003, **39**, 889-909.
2. B. A. Yankner, *Neuron*, 1996, **16**, 921-932.
3. E. R. Kandel, J. H. Schwartz and T. M. Jessell, *Principles of neural science*, McGraw-Hill, Health Professions Division, New York ; London, 4th ed. edn., 2000.
4. J. J. Hopfield and D. W. Tank, *Science*, 1986, **233**, 625-633.
5. E. Boldog, T. E. Bakken, R. D. Hodge, M. Novotny, B. D. Aevermann, J. Baka, S. Bordé, J. L. Close, F. Diez-Fuertes, S. L. Ding, N. Faragó, Á. Kocsis, B. Kovács, Z. Maltzer, J. M. McCorrison, J. A. Miller, G. Molnár, G. Oláh, A. Ozsvár, M. Rózsa, S. I. Shehata, K. A. Smith, S. M. Sunkin, D. N. Tran, P. Venepally, A. Wall, L. G. Puskás, P. Barzó, F. J. Steemers, N. J. Schork, R. H. Scheuermann, R. S. Lasken, E. S. Lein and G. Tamás, *Nature Neuroscience*, 2018, **21**, 1185-1195.
6. S. OGAWA, T. LEE, A. KAY and D. TANK, *Proceedings of the National Academy of Sciences of the United States of America*, 1990, **87**, 9868-9872.
7. C. S. Roy and C. S. Sherrington, *Journal of physiology*, 1890, **11**, 85-158.
8. 宮内，哲，*心理学評論*, 2013, **56**, 414-454.
9. M. Bresadola, *Brain Res Bull*, 1998, **46**, 367-380.
10. R. Caton, *Journal of Nervous & Mental Disease*, 1875, **2**.
11. M. Teplan, *Measurement science review*, 2002, **2**, 1-11.
12. A. Kiyohara, T. Taguchi and s. N. Kudoh, *The transactions of the Institute of Electrical Engineers of Japan. C, A publication of Electronics, Information and System Society*, 2009, **129**, 1815-1821.

13. D. Ito, H. Tamate, M. Nagayama, T. Uchida, S. N. Kudoh and K. Gohara, *Neuroscience*, 2010, **171**, 50-61.
14. J. Pine, *Journal of Neuroscience Methods*, 1980, **2**, 19-31.
15. G. W. Gross, B. K. Rhoades, H. M. Azzazy and M. C. Wu, *Biosensors and Bioelectronics*, 1995, **10**, 553-567.
16. D. Smetters, A. Majewska and R. Yuste, *Methods*, 1999, **18**, 215-221.
17. R. Kawakami, K. Sawada, A. Sato, T. Hibi, Y. Kozawa, S. Sato, H. Yokoyama and T. Nemoto, *Scientific Reports*, 2013, **3**, 1014.
18. F. Pascut, S. Kalra, V. George, N. Welch, C. Denning and I. Notingher, *Biochimica Et Biophysica Acta-General Subjects*, 2013, **1830**, 3517-3524.
19. 濱口宏夫, *日本分光学会測定法シリーズ 17*, 1988.
20. C. Raman, *Current Science*, 1998, **74**, 381-382.
21. Y. Komachi, T. Katagiri, H. Sato and H. Tashiro, *Applied Optics*, 2009, **48**, 1683-1696.
22. H. Sato, Y. Yamamoto, A. Maruyama, T. Katagiri, Y. Matsuura and Y. Ozaki, *Vibrational Spectroscopy*, 2009, **50**, 125-130.
23. Y. Oshima, H. Shinzawa, T. Takenaka, C. Furihata and H. Sato, *Journal of Biomedical Optics*, 2010, **15**.
24. K. Ajito, C. Han and K. Torimitsu, *Analytical Chemistry*, 2004, **76**, 2506-2510.
25. C. G. Dotti, C. A. Sullivan and G. A. Banker, *Journal of Neuroscience*, 1988, **8**, 1454-1468.
26. W. Yu and P. W. Baas, *Journal of Neuroscience*, 1994, **14**, 2818-2829.

Chapter 1

Analysis of the developing neural system using an in vitro model by Raman spectroscopy

Abstract

We developed an in vitro model of early neural cell development. The maturation of a normal neural cell was studied in vitro using Raman spectroscopy for 120 days. The Raman spectra datasets were analyzed by principal component analysis (PCA) to investigate the relationship between maturation stages and molecular composition changes in neural cells. According to the PCA, the Raman spectra datasets can be classified into four larger groups. Previous electrophysiological studies have suggested that a normal neural cell goes through three maturation states. The groups we observed by Raman analysis showed good agreement with the electrophysiological studies, except with the addition of a fourth state. The results demonstrated that Raman analysis was powerful to investigate the daily changes in molecular composition of the growing neural cell. This in vitro model system may be useful for future studies of the effects of endocrine disrupters in the developing early neural system.

1. Introduction

It is important to study the functions of neuron in order to understand mental activity and the neural system as a whole. Knowledge of neural systems may allow for the development of new therapeutic techniques for neurological diseases such as dementia and Parkinson's disease. In the present study, we employ an optical technique, Raman spectroscopy, instead of electrophysiological methods to investigate the relationship between molecular alterations and electrical activity in live growing neural cells in vitro. The central nervous system is mainly composed of two types of cells: neurons and glia cells. Although neurons are small in number of all cells, they are responsible for the essential functions of the brain, such as physical and emotional activities. The other cells, collectively called glia, provide support to the neural cells. Neurons generate electrical pulses even in the absence of external stimulation or during sleep.[1] This spontaneous neural firing is even observed in visual nerve cells of mouse embryos, although the cells have never been exposed to light.[2] Initially, this spontaneous firing was thought to be merely noise. However, the spontaneous firing was not just noise. Ikegaya et al. observed synchronized spontaneous firings of neocortical neurons in a live brain slice using a calcium imaging technique.[3] Kiyohara et al. used electrophysiology to investigate the relationships between evoked and spontaneous activity in a mature nerve cell model system cultured in a dish.[4] The nerve cells in the model system were collected from the hippocampus of a rat fetus. The researchers cultured the neural cells in a dish with multichannel electrodes, and observed the electrical properties of the live growing cells for around 80 days. The cells were silent for the first several days in vitro (DIV). Random electrical pulses were observed at 10 DIV, which were due to the unorganized spontaneous firing of the neural cells. After 60 DIV, synchronized "burst" signaling activity was observed, which suggested that the cells in the culture dish had formed a network. These results indicate that the neural cell undergoes at least three maturation states during the organization of an integrated system in the dish. The cell has an

independent state initially, following its differentiation from a neural stem cell. The cell gains the ability to fire electrical pulses randomly in the second state, and it begins making physical contacts with neighboring neural cells. In the third state, all cells in the dish have a greater degree of interaction with each other and are organized into one system. In this state, an electrical signal is efficiently transferred between cells resulting in a synchronized signal burst.

In the field of developmental psychology, researchers have recently begun to pay significant attention to endocrine disrupters. Some researchers have reported the effects of one particular endocrine disrupter, bisphenol A (BPA), on the behavior of children. BPA is an additive agent for plastics such as polycarbonate and epoxy resins. It has a structure similar to estrogen, and is able to bind to the estrogen receptor and disturbs estrogenic signaling pathways.[5] Zoeller et al. reported that BPA can also bind to the rat thyroid hormone (TH) receptor and act as an antagonist of TH, which is an essential hormone for normal brain development.[6] Further, Ishido et al. reported that 5-day-old rats exposed to 0.2 – 20 μg of BPA showed the typical symptoms of attention deficit hyperactivity disorder (ADHD).[7] These reports have emphasized the importance of studying the effects of endocrine disrupters on young neural cells in the early stages of brain development.

The purpose of the present study was to establish an in vitro model system that mimics the early stages of neural development, and to propose a method to monitor the response and maturation of cells by Raman analysis. Raman spectroscopy is a powerful technique to analyze live cells in vitro. For example, Oshima et al. successfully discriminated between four cancer cells and one normal cell by Raman spectroscopy without any sample treatments. In that study, principal component analysis (PCA) was used to discriminate the data groups.[8] Ghita et al. used Raman spectroscopy as a noninvasive, label-free technique to identify, image, and quantify potential molecular markers of neural stem cell differentiation status in vitro.[9] Raman spectroscopy is also

very powerful for long term observation because it is very low or no invasive to the live cells.[10,11] Using live giant squid axons, Nagashima et al. detected the unique coherent anti-Stokes Raman scattering (CARS) spectra of sevoflurane.[12] Ajito et al. employed a laser trapping technique with Raman analysis to observe the exocytosis of glutamic acid in a synaptosome isolated from a live neural cell.[13] The utility of Raman analysis for detection of viral infection in live cells has also been reported.[14] These previous reports reveal that multivariate analysis based on Raman spectroscopy is highly sensitive to any cellular changes due to external perturbations.

In the present study, we developed an in vitro neural development model system and analyzed its normal changes during the process of maturation. Animal models are not optimal for studying the effects of endocrine disrupters, because the in vivo neural system is highly complex and the small size of the mouse fetus makes experimental procedures difficult. Moreover, the cost and time for each experiment is substantial, because it is necessary to sacrifice an animal at every time point for measurements. In contrast, studying an in vitro model system with Raman analysis is simple and less costly. In this system, the researcher can observe the state of cells repeatedly by Raman analysis without causing any cellular damage. Neural cells undergo significant changes during the stages of maturation, and it is important to collect basic data regarding the normal maturation states of cultured cells. In the future, the present Raman analytical method and basic knowledge of cell maturation states can be extended to 3D cultured nerve systems and/or live brain slice models with new Raman imaging technologies.[15-18]

2. Materials and methods

2.1 Primary culture of rat hippocampal neural cells

The hippocampus was dissected from the brains of Wistar rats (CLEA Japan, Tokyo) at embryonic day 18. The dura mater and other surrounding tissues were carefully removed, and the hippocampus was washed three times with Ca^{2+} and Mg^{2+} free

phosphate buffered saline (PBS(−), Life Technologies, New York City). This procedure eliminated potential fibroblast contamination from the dura mater and other surrounding tissues. Hippocampal neurons were dissociated into single cells by treating them with 0.125% trypsin-EDTA (Wako, Osaka) in PBS(−) at 37 °C for 10 min. The cells were rinsed with PBS(−) three times and transferred into 2 mL of culture medium. The culture medium consisted of Neurobasal A medium (Life Technologies, New York City) with 0.5 mM L-glutamine, B27 supplement, and 100 Units mL^{-1} of penicillin–streptomycin. The cell density was 100,000 cells mL^{-1}. The suspension was transferred into a 35 mm polyethyleneimine-coated dish with a quartz window at the bottom (Fine Plus International, Kyoto). Ten dishes of sample were prepared from about 10 embryos obtained from one rat. The cells were cultured in an incubator at 37 °C with 5% CO_2 and saturated humidity. Half of the culturing medium was changed every 3 days. The Raman measurements were carried out at 2, 8, 15, 30, 45, 60, 75, 90, 105, and 120 days after the cell seeding. The sample was discarded after every measurement because there was possibility of contamination during the measurement. This study was approved by the Institutional Animal care and Use Committee of Kwansei Gakuin University (Sanda, Japan).

2.2 Immunostaining

Immunostaining was carried out for the microscopic observation of neural cells. The cells were cultured for 120 days, and were stained following the Raman measurement. The cells were washed twice in PBS(−), then fixed with methanol (Wako, Osaka) at −20 °C for 10 min. The methanol was washed out by soaking the sample in PBS(−) three times for 5 min each time. The fixed cells were treated with TritonX-PBS (0.2%) for 1 min to permeabilize the membranes, then blocked with goat serum (10%) at 37 °C for 1 h. The sample was treated with rabbit polyclonal MAP2 antibody (1:1000; EMD Millipore, Burlington) and mouse IgG_1 monoclonal GFAP antibody (3 μg mL^{-1}; Sigma-

Aldrich, St. Louis) at 37 °C for 2 h. After treatment with the primary antibodies, the sample was washed with PBS(−) three times for 5 min each. The secondary antibodies were Alexa Fluor® 546 conjugated anti-rabbit IgG and Alexa Fluor® 647 conjugated anti-mouse IgG_1 (Life Technologies, New York City), and treatment was conducted in the dark for 1 h at room temperature. The cell nuclei were stained with 4′,6-diamidino-2-phenylindole (DAPI; SouthernBiotech, Alabama). Fluorescent images were observed with an A1 confocal fluorescence microscope (Nikon, Tokyo).

2.3 Raman spectroscopy

Raman spectra were measured with a confocal micro-Raman system (Nanofinder30, Tokyo Instruments, Tokyo) with a CO_2 incubating sample holder as shown in Fig. 1. The system was equipped with a 600 lines mm^{-1} grating (blazed at 750 nm), CCD cooled to −80 °C (DU420-BRDD; Andor Technology, Belfast), and continuous-wave background-less electrically tuned Ti: Sapphire laser (CW-BL-ETL) which provided excitation light at 785 nm.[19] The excitation laser was focused by a 60× water immersion objective lens (N.A. 1.1, LUMFLN; Olympus, Tokyo). The power was typically 35 mW at the sampling point. The lateral and vertical spatial resolutions were estimated to be 1 and 5 μm, respectively. The Raman measurement acquisition time was 90 s. The Raman scattered light was collected at the back scattered configuration. The background spectra of quartz and culture medium were subtracted from the spectra. Further background correction was carried out by subtracting the 11th-order polynomial-fitted background to remove baseline undulation. Spectra were normalized with a standard band at 1450 cm^{-1}, which is assigned to the CH_2 deformation mode,[20] prior to the multivariate analysis. The Raman spectra were analyzed with The Unscrambler multivariate analysis software (Camo, Oslo).

3. Result and discussion

3.1 Morphological observation of cell growth

For the Raman measurement, an area of cultured cells with a suitable density was selected. Bright field images of cultured neural cells at 2, 15, 60, and 90 DIV are shown in Fig. 2(a)–(d). There were neural and glial cells in the dish, and no fibroblasts were observed in the 2 DIV image (a). The neural cell (solid arrow) has a well-defined nucleus and looks sharp. In contrast, the glial cell (dotted arrow) shows flat stubby feature and no defined nucleus. At this point, the neural cell was in the G_0 state and ceased to proliferate.[21] The cell body, axon, and dendrites grew considerably from 2 to 15 DIV, but the cell density in the dish was still relatively low. At 60 and 90 DIV, the neural cells further extended their axon and dendrites to construct a network. There was a higher density of both glia and neural cells, such that their cell bodies overlapped. No fibroblasts were seen in the culture. Considering fibroblasts proliferate quickly, within 10 days they would occupy most of the space in the dish when seeded with G0 phase neurons. Thus, their absence suggests that the sample preparation procedure was effective. Glial cells have features similar to those of neural cells, but lack an axon. Since it is necessary to visually select a neural cell for the Raman measurement, the cell density should not be too high. However, the neural cell needs to have intercellular connections to correctly build a network. We investigated the optimal cultured cell density for Raman observation. In the present study, the initial cell density seeded into the dish was approximately 250 cells mm^2.

Pseudo-colored immunostained images of the neural cell at 120 DIV are shown in Fig. 2(e). The cells were stained with antibodies against MAP2 and GFAP. The MAP2 (green) protein exists in the neural cell body and dendrites, and GFAP (red) is found in the cell body of the astrocyte. The nucleus was stained with DAPI (blue). The axon of the neural cell was not visible in the image because it lacks MAP2. The cell bodies of oligodendrocytes and microglial cells were also not observed because they lack GFAP. Neural cells have a larger nucleus than glia, and the neural cell body is surrounded by

astrocytes, which regulate synaptic transmission and supply energy to these cells.[22] Some isolated blue spots may represent the nuclei of oligodendrocytes, which form the myelin sheath around the axon, and microglia, which act as immune cell-like scavengers in the brain.

3.2 Raman analysis

Raman spectra were collected only from the neural cells. It was easy to discriminate the neural cells from the glial cells by visual selection in bright field images as shown in Fig. 2. We focused the laser on the nucleus, cytoplasm, and dendrites to measure and compare the respective spectra (Fig. 3). Results indicated that the nuclear spectra were of much higher quality than the spectra of the cytoplasm and dendrites. Hence, the nuclear spectra were used for analysis in this study. Averaged Raman spectra of cells cultured for 2, 8, 15, 30, 45, 60, 75, 90, 105, and 120 DIV are shown in Fig. 4(a)–(j). The intensity of the spectra were normalized with the standard band at 1450 cm^{-1}, which is assigned to the CH_2 and CH_3 bending modes. This reflects the amount of CH bonding in all organic materials in the cell. A band at 785 cm^{-1} was assigned to DNA, which was observed most strongly in the 2 DIV spectrum. Bands at 1663 and 1339 cm^{-1} were assigned to amide I and amide III modes of proteins. A band at 1251 cm^{-1} arose from the amide III mode of proteins and the C=CH mode of lipids. The intensity of the band reflects the concentration of material included in the excitation volume of the focal point. The neural cell did not proliferate in the present culturing condition, meaning no duplication of DNA had taken place. As observed in the microscopic image, the size of the nucleus was smallest at 2 DIV compared to the other culturing days. This indicates that the DNA density was highest in the neural cell at 2 DIV, because the total molecular weight of DNA was static. According to the subtraction (The data were not shown.), the bands at 1093 and 1003 cm^{-1} showed a reduced intensity when the cells were cultured longer. They arose from phenylalanine and DNA, respectively. As the neural cell does not

proliferate and the cell cycle is arrested at G_0, these molecular changes were attributed to the growth of the neural cell. A spectrum (k) in Fig. 4 is the averaged spectrum of cytoplasm. The band at 785 cm^{-1} due to DNA is missing. As it has lower signal-to-noise ratio, we did not use the spectra of cytoplasm in the detailed analysis.

PCA was applied to analyze the results in more detail. PCA score plots for PC1, 2, and 3 are depicted in Fig. 5. The datasets for the 10 groups of different cell culture DIV lengths are exhibited in the plots. It should be noted that data in this PCA include the spectra obtained in the three totally independent experiments. There is no clear segmentation observed within each dataset. It suggests high reproducibility and reliability of the present results. The analysis showed that there were four main data groups: (α) 2 DIV, (β) 8–30 DIV, (γ) 45–105 DIV, and (δ) 120 DIV. The α group consisted of the youngest cells and showed good separation from the β group, suggesting that the young neural cells undergo large changes at the beginning of their maturation process. This group represents the earliest stage of the neural cell after its differentiation from the neural stem cell. In this stage, the cell has no electrical activity, and its axon and dendrites grow quickly. The β group appears to be a transient state. The datasets from different cultivation days were dispersed within this group, but were independent from the other data groups. This group may correspond to the second stage of the neural cell maturation. During this stage, the neural cell shows spontaneous and random firing of electrical pulses. According to the previous electrophysiological study, this stage generally lasts from 10 to 60 DIV. Our Raman analysis detected the transition from the first stage to the second stage slightly earlier than that seen in the electrophysiological observations. Cells belonging to the γ group are relatively stable, because the datasets from different cultivation days overlap with each other in the score plots. Neural cells cultured in vitro generally show synchronized signal burst firing after 60 DIV according to electrophysiological observations, and the present Raman observations are in accordance. The last group, δ, consists only of the dataset from 120 DIV. This group is clearly isolated from the other

groups, particularly in PC3 and does not have a corresponding state observed in the electrophysiological study.

The loading plots of PC1 (a), PC2 (b), and PC3 (c) are shown in Fig. 6. The datasets for 2 and 8 DIV have a relatively higher value in PC1 in the score plots (Fig. 5). The PC1 loading plot had strong bands at 788, 1095, 1487 and 1576 cm^{-1}, which were assigned to DNA. This revealed that PC1 reflects the concentration of DNA in the nucleus, because young cells have a relatively smaller nucleus. In contrast, the groups γ and δ had a relatively high value on the PC2 axis. The PC2 loading plot showed slightly more complicated features, and there were small bands in the plot that were difficult to assign. The bands assigned to phenylalanine appeared strongly at 1003 and 1031 cm^{-1}, suggesting that protein species expression differed in mature and young cells. The PC3 axis seemed to reflect the maturation of the neural cells, except for the dataset of 2 DIV. A band at 893 cm^{-1} may be assigned to the C–C skeletal mode of lipids. Negative features at 1664, 1307 and 1260 cm^{-1} are assignable to CvC stretching, CH_3/CH_2 twisting or bending mode, and C=C–H bending modes of fatty acid chains in lipids. Positive bands at 1441 and 1414 cm^{-1} were thought to reflect structural changes to the backbone to which the CH_2 and CH_3 groups belong. The band at 1330 cm^{-1} was attributed to phospholipids.[23] In summary, these results suggested that compositional changes in lipids take place during the neural cell maturation process. The neural cell initially accelerates growth to extend its axon and dendrites after settling on the dish, and its growth gradually slows down along with the organization of neural system. The cell may need to have a more flexible cytoplasmic membrane with a specific composition of phospholipids during the active maturation phase. Each neighboring two datasets of different culturing date were analyzed with partial least square regression (PLSR)[24,25] in order to clarify the trends of spectral changes. The factors to discriminate two groups in Fig. 7 were mostly admixture of PC1, 2 and 3 in Fig. 6. The only factor between 105 and 120 DIV (Fig. 7) was not similar to any of them, suggesting that the neural cell makes a characteristic alteration in

the δ stage. However, the function and/or character of the cell in this stage is totally unknown at present.

4. Conclusion

The spectral changes of a live growing neural cell were successfully analyzed in the present study. The datasets were classified into 4 groups that reflect the maturation states of the neural cell. The first group consists of the 2 DIV dataset, in which the neural cell has a small nucleus with condensed DNA. The 2 DIV neural cell generally does not show any electrical activity. The second group includes the 8–30 DIV datasets. At this stage, the cell grows actively and has a slightly different composition of lipid species. This group seems to correspond to the maturation stage of random spontaneous signaling. The third group consists of the 60–90 DIV datasets. The cells in this state showed very similar Raman spectra, indicating that their molecular composition was stable. The fourth group consists of only the 120 DIV dataset. According to the PCA, the lipid composition of the cell at 120 DIV was more similar to that of the cell at 2 DIV. Electrophysiological studies suggest that the neural cells organize into a large system and show signal bursts in the third and fourth groups. Our results indicate that Raman spectroscopy is a powerful noninvasive tool to analyze the maturation stages of neural cells. This method provides information on the molecular composition of live cells without any staining or labeling. In the present study, we succeeded in generating a model dataset that mimics the normal growth of developing neural cells. The response of developing neural cells to endocrine disrupters can be analyzed by a comparison with this model.

References

1. D. A. McCormick, *Science*, 1999, **285**, 541-543.
2. M. Weliky and L. C. Katz, *Science*, 1999, **285**, 599-604.
3. Y. Ikegaya, G. Aaron, R. Cossart, D. Aronov, I. Lampl, D. Ferster and R. Yuste, *Science*, 2004, **304**, 559-564.
4. A. Kiyohara, T. Taguchi and s. N. Kudoh, *The transactions of the Institute of Electrical Engineers of Japan. C, A publication of Electronics, Information and System Society*, 2009, **129**, 1815-1821.
5. N. Ben-Jonathan and R. Steinmetz, *Trends in Endocrinology and Metabolism*, 1998, **9**, 124-128.
6. R. Zoeller, A. Dowling, C. Herzig, E. Iannacone, K. Gauger and R. Bansal, *Environmental Health Perspectives*, 2002, **110**, 355-361.
7. M. Ishido, Y. Masuo, M. Kunimoto, S. Oka and M. Morita, *Journal of Neuroscience Research*, 2004, **76**, 423-433.
8. Y. Oshima, H. Shinzawa, T. Takenaka, C. Furihata and H. Sato, *Journal of Biomedical Optics*, 2010, **15**.
9. A. Ghita, F. Pascut, M. Mather, V. Sottile and I. Notingher, *Analytical Chemistry*, 2012, **84**, 3155-3162.
10. A. Ghita, F. C. Pascut, V. Sottile and I. Notingher, *Analyst*, 2014, **139**, 55-58.
11. F. C. Pascut,S. Kalra,V. George,N. Welcha,C. Denning and I. Notingher, *Biochimica et Biophysica Acta*, 2013, **1830**, 3517–3524.
12. Y. Nagashima, T. Suzuki, S. Terada, S. Tsuji and K. Misawa, *Journal of Chemical Physics*, 2011, **134**.
13. K. Ajito, C. Han and K. Torimitsu, *Analytical Chemistry*, 2004, **76**, 2506-2510.
14. K. Moor, K. Ohtani, D. Myrzakozha, O. Zhanserkenova, B. Andriana and H. Sato, *Journal of Biomedical Optics*, 2014, **19**.

15. Y. Oshima, C. Furihata and H. Sato, *Applied Spectroscopy*, 2009, **63**, 1115-1120.
16. Y. Oshima, H. Sato, H. Kajiura-Kobayashi, T. Kimura, K. Naruse and S. Nonaka, *Optics Express*, 2012, **20**, 16195-16204.
17. K. Shi, P. Edwards, J. Hu, Q. Xu, Y. Wang, D. Psaltis and Z. Liu, *Biomedical Optics Express*, 2012, **3**, 1744-1749.
18. A. Silve, N. Dorval, T. Schmid, L. Mir and B. Attal-Tretout, *Journal of Raman Spectroscopy*, 2012, **43**, 644-650.
19. H. Sato, S. Wada and H. Tashiro, *Applied Spectroscopy*, 2002, **56**, 1303-1307.
20. Z. Movasaghi, S. Rehman and I. Rehman, *Applied Spectroscopy Reviews*, 2007, **42**, 493-541.
21. E. Lee, N. Hu, S. Yuan, L. Cox, A. Bradley, W. Lee and K. Herrup, *Genes & Development*, 1994, **8**, 2008-2021.
22. P. Magistretti, L. Pellerin, D. Rothman and R. Shulman, *Science*, 1999, **283**, 496-497.
23. R. Malini, K. Venkatakrishna, J. Kurien, K. Pai, L. Rao, V. Kartha and C. Krishna, *Biopolymers*, 2006, **81**, 179-193.
24. J. Trevisan, J. Park, P. P. Angelov, A. A. Ahmadzai, K. Gajjar, A. D. Scott, P. L. Carmichael and F. L. Martin, *Journal of Biophotonics*, 2014, **7**, 254-265.
25. M. J. Walsh, A. Hammiche, T. G. Fellous, J. M. Nicholson, M. Cotte, J. Susini, N. J. Fullwood, P. L. Martin-Hirsch, M. R. Alison and F. L. Martin, *Stem Cell Research*, 2009, **3**, 15-27.

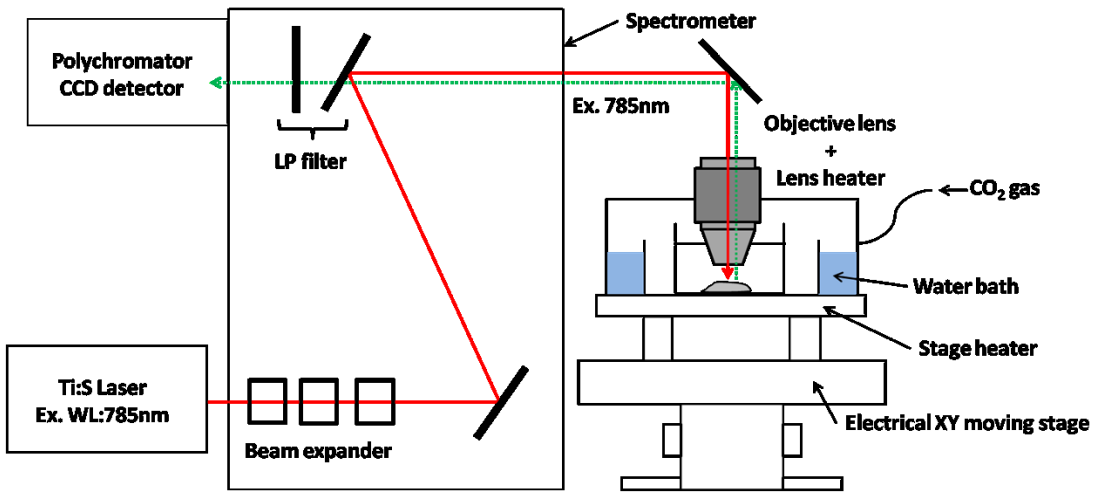

Figure 1

Scheme of the confocal Raman microscope equipped with a CO_2 incubator.

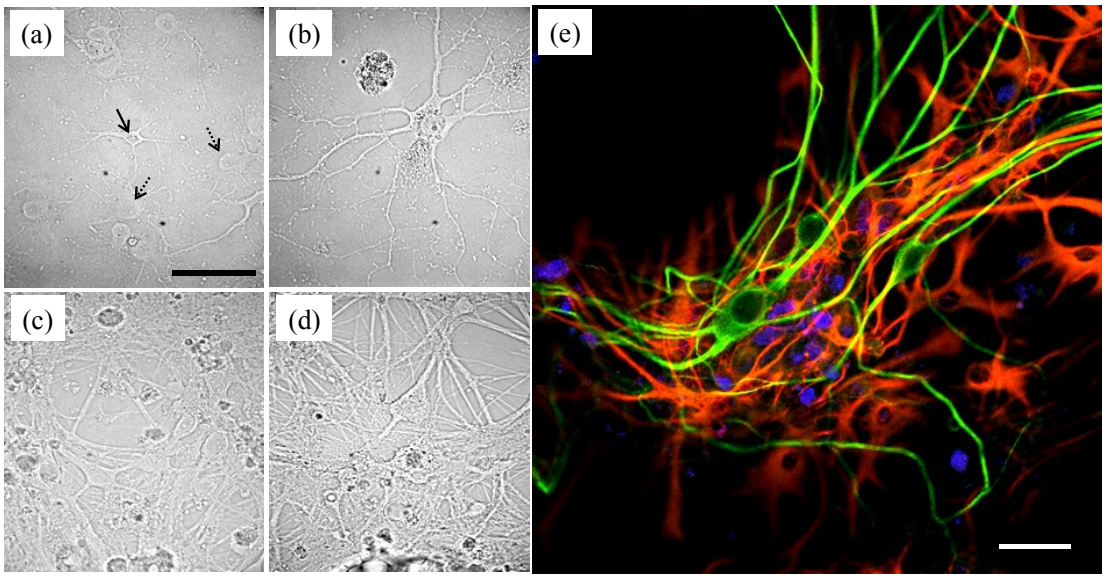

Figure 2

Bright field images of the cultured neural cells at 2 days in vitro (DIV) (a), 15 DIV (b), 60 DIV (c), and 90 DIV (d). A fluorescent image of immu- nostained neural cells at 120 DIV is shown in (e). Cells were stained with MAP2 (green), GFAP (red) and DAPI (blue). The scale bars in (a) and (e) indicate 50 μm. The solid arrow and dotted arrow in image (a) point at neural and glia cells, respectively.

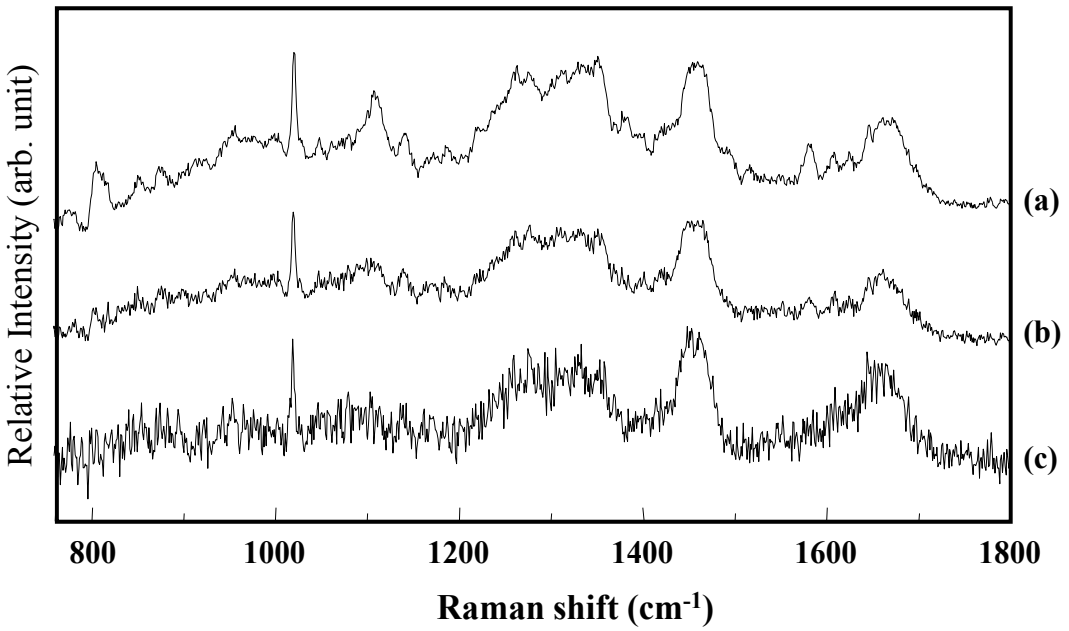

Figure 3

The averaged spectra obtained from (a) nuclei, (b) cytoplasms and (c) neurites of neural cells at 15 DIV. (n = 30)

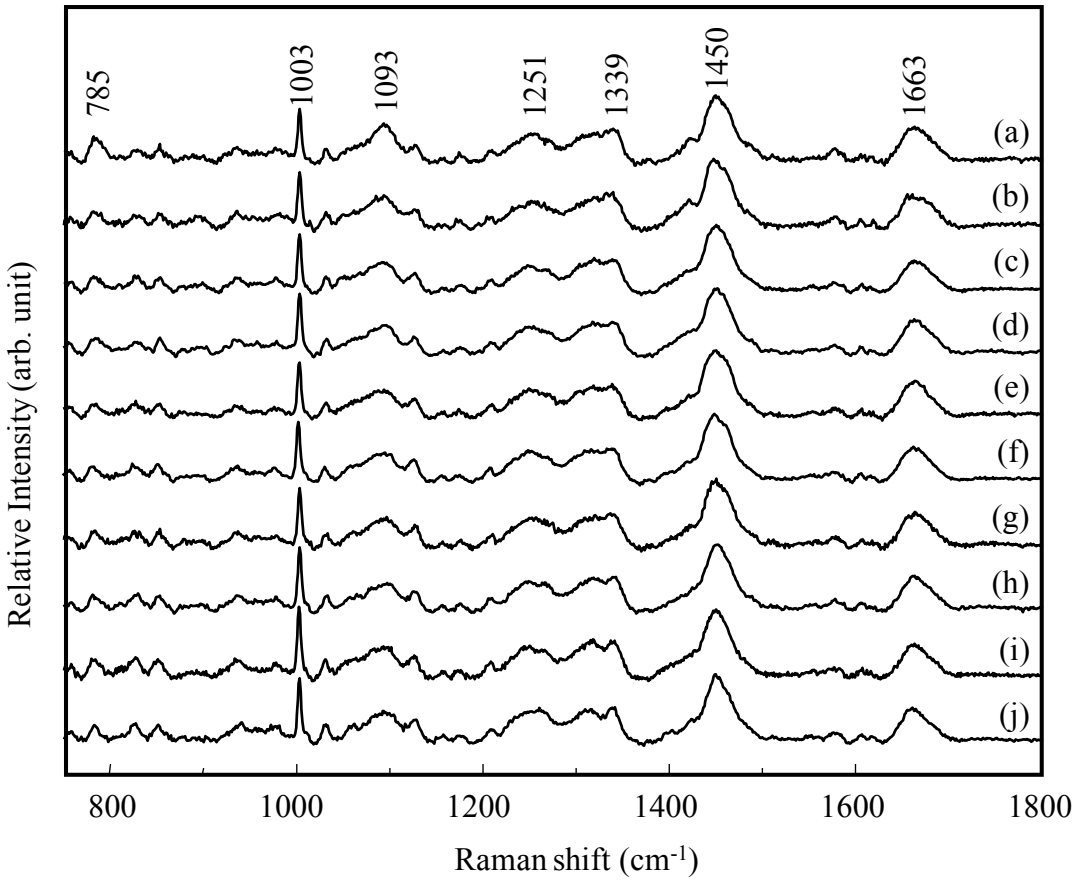

Figure 4

Averaged spectra of the neural cells measured at (a) 2 days in vitro (DIV), (b) 8 DIV, (c) 15 DIV, (d) 30 DIV, (e) 45 DIV, (f) 60 DIV, (g) 75 DIV, (h) 90 DIV, (i) 105 DIV, (j) 120 DIV.

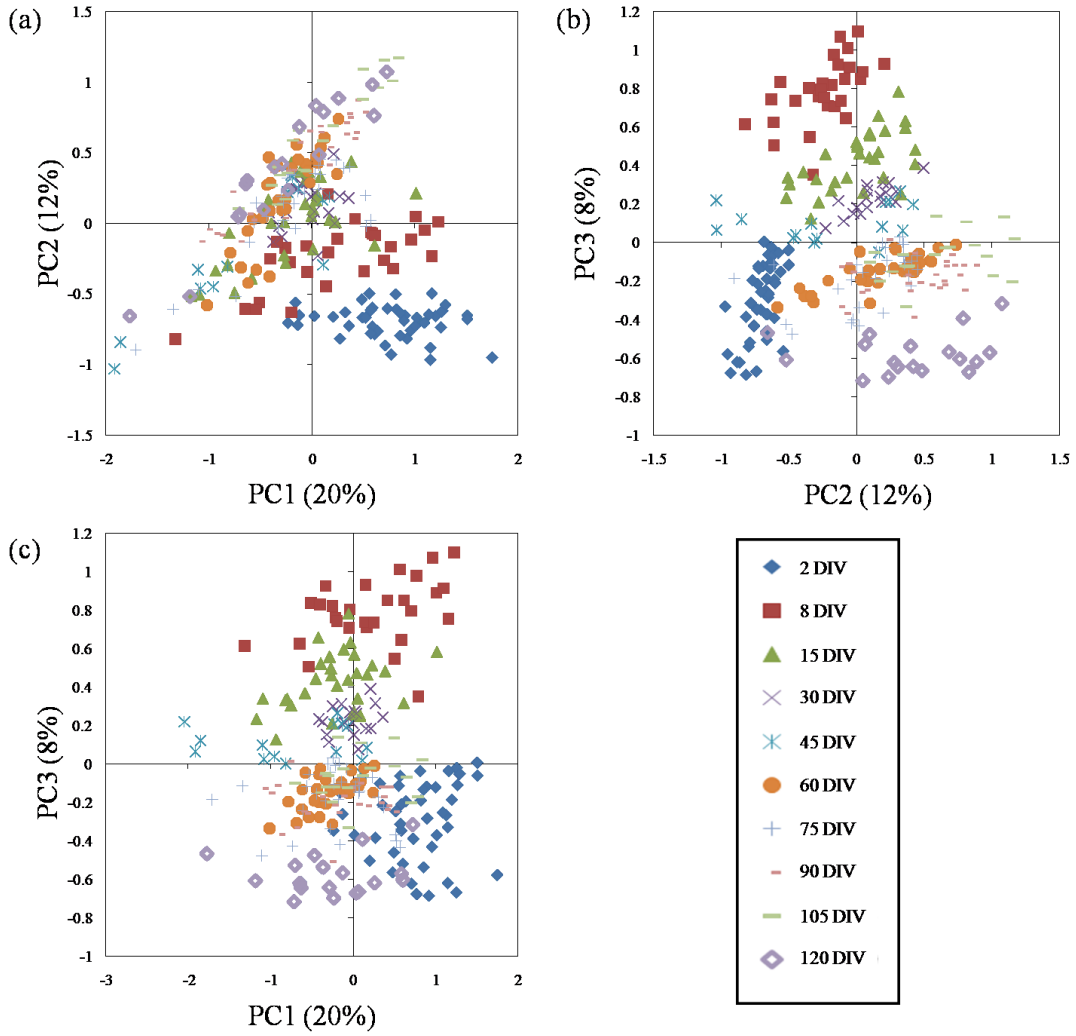

Figure 5

Principal component analysis (PCA) score plots of the datasets for (a) PC1 vs. PC2,

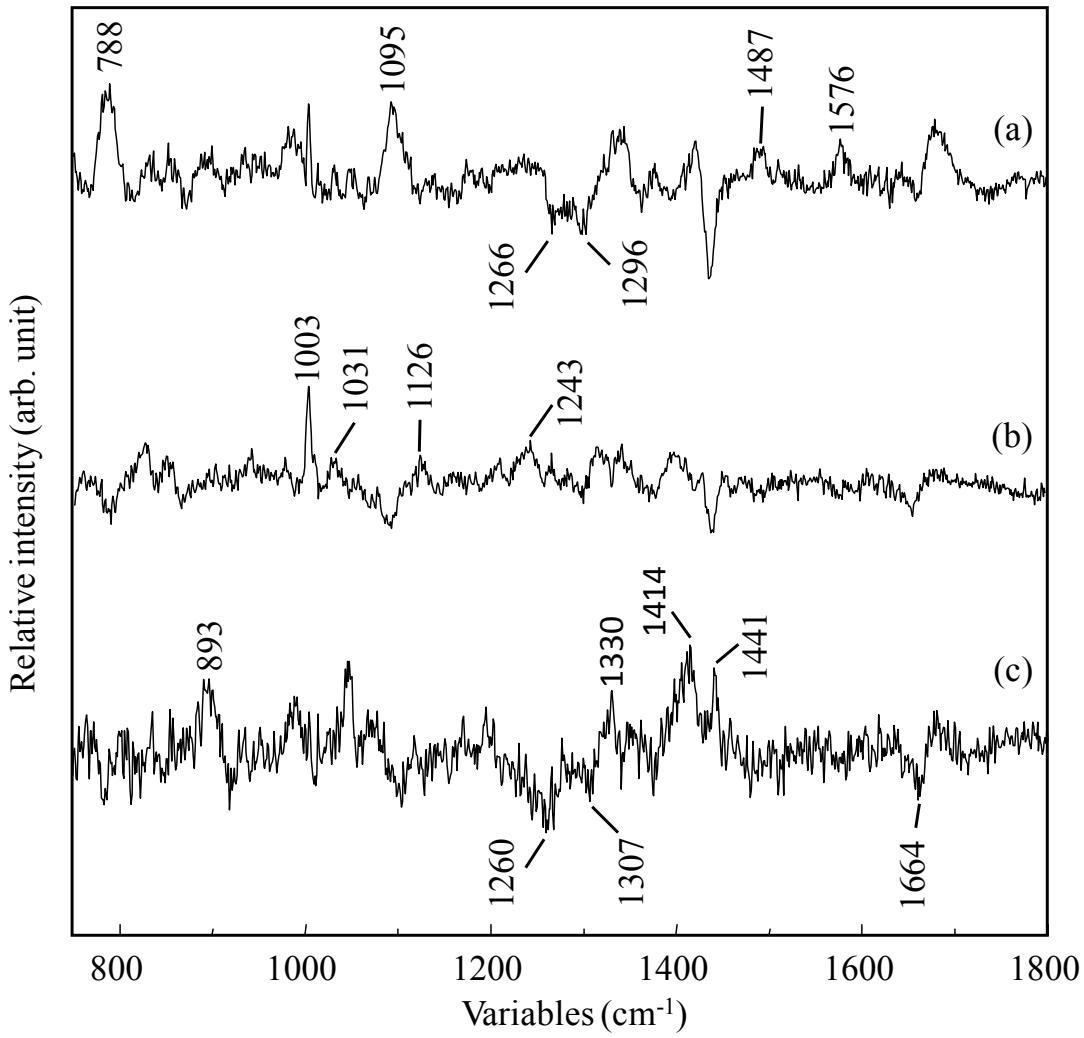

Figure 6

PCA loading plots of (a) PC1, (b) PC2 , and (c) PC3.

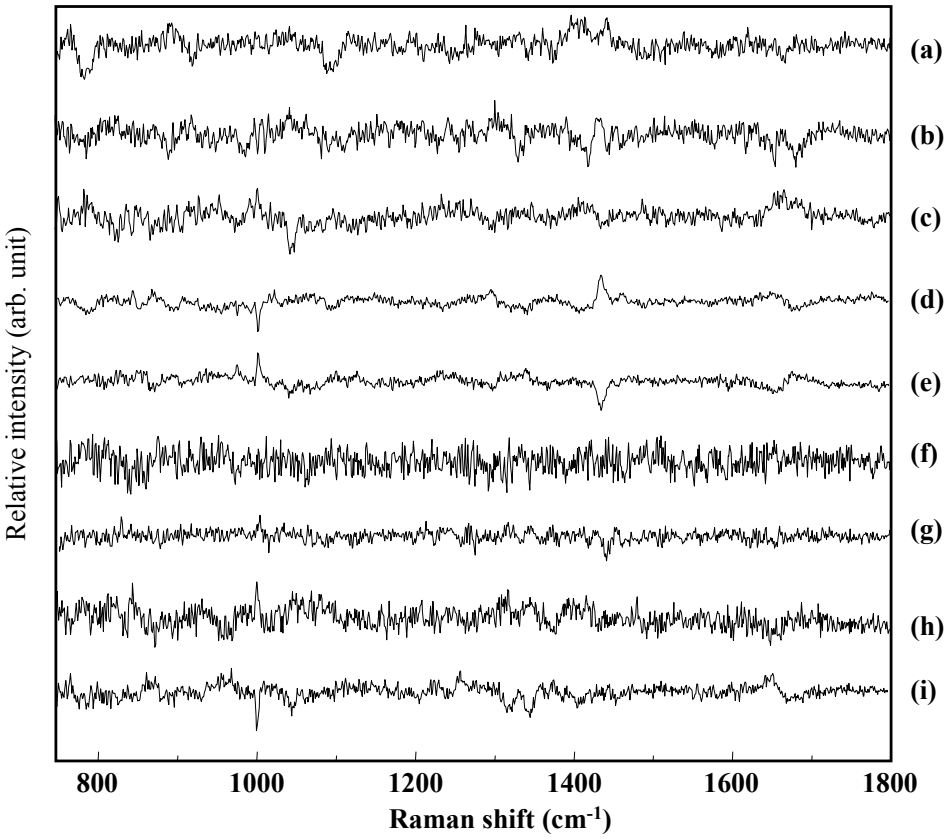

Figure 7

The factors for discrimination of each neighboring two datasets of different DIVs datasets caluculated by PLSR. (a) 2 DIV vs. 8 DIV, (b) 8 DIV vs. 15 DIV, (c) 15 DIV vs. 30 DIV, (d) 30 DIV vs. 45 DIV, (e) 45 DIV vs. 60 DIV, (f) 60 DIV vs. 75 DIV, (g) 75 DIV vs. 90 DIV, (h) 90 DIV vs. 105 DIV, (i) 105 DIV vs. 120 DIV.

Chapter 2

Discrimination analysis of excitatory and inhibitory neurons using Raman spectroscopy

Abstract

We have succeeded in discriminating between intact excitatory and inhibitory neural cells with Raman analysis. Excitatory and inhibitory neurons have several differences in their electric activities, but it can be difficult to determine their types based only on visual appearances. As Raman spectroscopy does not require any staining or labeling, its use in live neural cells is possible. In the present study, we used primary neurons obtained from rat cerebral cortexes, which we cultured on a glial feeder layered culturing dish for 15 days. The Raman spectra of the intact neurons on the dish were obtained; the neurons were then immunostained and their types determined. Partial least squares regression-discriminant analysis (PLSR-DA) was employed for classification of the excitatory and inhibitory neurons. The results demonstrated a high feasibility for use of Raman spectroscopy for discrimination analysis of inhibitory and excitatory neurons in a nondestructive manner.

1. Introduction

The brain mainly consists of neurons and neuroglial cells. Neurons are small units of the neural network that receive, integrate, and send signals in order to control the body's actions. Neuroglial cells modulate neural signal transmission, although they do not have a direct role in synaptic interaction. While both neurons and neuroglial cells are necessary to maintain the total nervous system, neurons also play a major role in information processing.[1] A neuron has single long neurite and is therefore relatively easy to visually identify on microscopic observation, even when among other cells. Morphological changes of a neuron during neural polarization have been studied,[2] and it was revealed that one of the neuron's lamellipodia becomes the axon and the others become dendrites.[3] Neural cells have numerous connecting points between the synapses on the axon and the dendrites on the cell body, and the electric signal is transferred in one direction, from the presynaptic cell to the postsynaptic cell, through these connecting points. One neuron receives signals from 100,000 other neural synapses. The neuron is classified into two types according to neurotransmission: (1) an excitatory neuron that secretes glutamic acid for a neurotransmitter at a synapse in order to induce action potential in postsynaptic cells, and (2) an inhibitory neuron that secretes γ-aminobutyric acid (GABA) to decrease action potential. These two simple synaptic transfers constitute the complex functions of the central nerve system (CNS).[4] Although the functions of these two types of neurons are quite different, it can be difficult to discriminate them because of the similarity in their shapes. Staining using an immune-enzymatic technique has been performed to discriminate between them;[5] however, it can be difficult to apply the immunostaining technique to live neurons without interfering with their actions.

Kiyohara et al. reported that, without any external stimulation, cultured neural cells form an autonomous network system that covers a whole culture dish.[6] The study indicated that a cultured neural network is a good model to use when studying the functions of neurons in a network. Previous electrophysiological studies suggested that

the cultured neurons showed spontaneous signaling on day 10 and organized periodical signals on day 30–60 in the dish.[7] Remarkable changes appeared in the spectra obtained near the 8th and 45th days under cultivation, suggesting that specific molecular changes preceded functional changes in the neuron.[8] Although the developing neuron has been studied using electrophysiological methods, Raman spectroscopy is able to provide new insight into the neural science.

To analyze the neural circuit in the culture dish in more detail, it is necessary to determine the excitatory and inhibitory neurons in a fully noninvasive manner, to gain a better understanding of the neural network system. An immunostaining method is generally used for discrimination analysis, but when using this method, fixing the cell is unavoidable. A technique using fluorescent proteins has been used to discriminate between live excitatory and inhibitory neurons.[9] However, the fluorescent proteins sometimes interfere with the natural function and localization of the target protein because they can lead to misfolding of the fused protein or suppression of the correct transportation.[10,11] According to previous studies, differentiation of excitatory and inhibitory cells has been possible through observation of axonal formations. For example, Hayashi et al. reported that speed of the axonal extension is different between excitatory and inhibitory neurons.[12] The excitatory neuron formed axons within 3 days of culturing, but the inhibitory neuron took more than 6 days to form axons. Cell density on the culture dish must be regulated correctly for visual discrimination to take place, because the axon and dendrites make a complicated network. A lower cell density is better to observe the shape of a single neuron, but a cell with a lower density often lacks synchronized signaling activity. Sufficient cell density is therefore necessary to create the functional network. For example, when the cell density is less than 250 cells per mm^2, signaling was not observed even after long-term cultivation.[7] However, overlapping axons and dendrites make it difficult to observe the shape of a single cell. Hence, it is difficult to discriminate between excitatory and inhibitory neurons in a live neural network system using

conventional methods, especially visual observation.

The purpose of this study is to develop a technique to discriminate between excitatory and inhibitory neurons using Raman spectroscopy, without any labelling or morphological observation. It provides information regarding the molecular composition of live cells noninvasively and in real time.[13–15] The combination of Raman spectroscopy and chemometrics has a high potential for use in the biological field,[16] such as in diagnosis, monitoring of cell differentiation, and apoptosis.[17–19] Classification using partial least squares regression-discriminant analysis (PLSR-DA) has high accuracy.[20–23] Heraud et al. suggested that Raman spectroscopy enabled in vivo analysis of nutrient status in single microalgae cells.[24] Classification of the N-replate and N-starved cells was performed using PLSR-DA. Bergholt et al. demonstrated how to classify different gastric tissue types using PLSR-DA.[25] Taketani et al. performed in situ detection of early-stage colorectal cancer using a ball lens-mounted hollow optical fiber Raman probe.[17,26] In this study, we demonstrate the potential of Raman spectroscopy for discrimination between excitatory and inhibitory neurons in live cells under culture conditions. A low-density culturing procedure has been developed to observe single neurons using Raman spectroscopy as well as the immunostaining method. The PLSR-DA technique with leave-one-out cross-validation was performed to build and optimize the discriminant model.

2. Material and methods

2.1 Animal preparation

Experiments were performed using Wistar rat fetuses between 17 and 19 days of gestation. This study was approved by the Institutional Animal Care and Use Committee of Kwansei Gakuin University (Sanda, Japan) and care and handling of animals were in accordance with the guidelines of the committee in full compliance with Act on Welfare and Management of Animals (Act No. 46 of May 30, 2014) and Standards relating to the Care and Keeping and Reducing Pain of Laboratory Animals (Notice of the Ministry of

the Environment No. 84 of 2013).

2.2 Sample preparation

A glial cell feeder layer was used to nourish the low-density neurons. Cells containing neurons and glia were obtained from the cerebral cortex of rat embryos at 18 days of gestation. The pia mater of the brain was peeled off, and the cerebral cortex was rinsed with Ca^{2+}- and Mg^{2+}-free phosphate buffered saline (PBS(−)). The tissue was transferred into a 15 mL centrifuge tube and treated with 0.5 mM papain (Funakoshi) at 37 °C for 30 min. After the treatment, papain was deactivated with 10% fetal bovine serum (FBS) in PBS(−). The tissues were rinsed with PBS(−) three times and transferred into 2 mL of culture medium. Minimum essential medium (MEM, Invitrogen) was employed as the basal medium, with supplements including 3.65 mg of L-glutamine (Invitrogen), 180 mg of glucose (Wako), 5 μg of epidermal growth factor (EGF, Invitrogen), and 2.5 ml of FBS (Invitrogen) for 50 ml of the medium. The cerebral cortex tissue was dissolved into single cells by gentle suspension, which were then cultured in a 75 cm^2 flask (Corning) at 37 °C in an atmosphere of 95% air/5% CO_2. The medium was changed every 7 days during the culturing period. After 14 days, the cells in the flask were mostly glial cells, because neurons do not proliferate. The cells were treated with 0.05% trypsin-EDTA for 3 min, and then they were collected by centrifugation again. The glial cells in suspension (7500 cells per mL × 110 μL) were seeded onto a quartz-bottom dish, allowed to stand for 24 hours for cell settlement, and then treated with 2 mL of culture medium. The glial cells covered the dish as a single confluent layer in a week. Neurons were collected from the occipital lobes of rat embryos at 18 days of pregnancy. The procedure used to extract neurons was similar to that used for glial cells, as described above. Rather than culturing the neurons in the flask, we seeded both the suspension of mixed cells and the dissolved occipital lobe tissue on a culture dish with the glial cell feeder layer at density of 40 cells per mm^2 and allowed them to culture for 2 days. The

neuron was then exposed to 5 μM cytosine β-D-arabinofuranoside (Ara-C) for 24 hours in order to remove glial cells that were included in the newly seeded cells. When Ara-C induces apoptosis for the mitotic cell, the glial cells coexisting with the neuron are eliminated. The glial cells in feeder layer have already stopped proliferation by the time of this treatment. The neuron is not affected by Ara-C, because the cell cycle ended when it underwent neural differentiation. Therefore, only neurons were left on the glial feeder layers. The neuron was cultured in a Neurobasal A (Invitrogen) medium with supplements 0.5 mM L-glutamine (Invitrogen), B27 supplement (Invitrogen), and 100 units per mL of penicillin–streptomycin (Invitrogen) for 15 days.

2.3 Raman spectroscopy and data pre-treatment

Since determination of the neuron type was conducted by immunostaining after the Raman measurement of live cells, it was necessary to identify each cell for the analysis on the culture dish. We drew gridlines and markers beneath the quartz window of the dish and recorded the shape and location of each cell before the Raman measurement. The Raman spectra were obtained from the nuclei of the neurons. The confocal Raman microscope system (Nanofinder30, Tokyo instruments) had a 60× water immersion objective lens (N.A. 1.1, LUMFLN, Olympus), CO_2 chamber (Tokai hit), and an XY motor driven stage (Chuo precision industrial). This motor driven stage was controlled with 1 μm step. The system included a spectrometer equipped with a 600 lines per mm grating (blazed at 750 nm) and a water-cooled CCD (driven at −80 °C; DU420-BRDD; Andor Technology). An excitation light at 785 nm was provided from a continuous-wave background-less electrically tuned Ti:Sapphire laser (CW-BL-ETL).[27] The laser power was 30 mW at the sampling point, and the acquisition time was 90 s. The spot size of laser was approximately 1 μm diameter on a plane and the focal depth was estimated 5 μm.

The Raman-scattered light in a region of 760–1800 cm^{-1} was collected at the

back-scattered configuration. Background spectra were recorded from the neuron at the same height of laser focus. After subtraction of the background spectra, all data were smoothed using the Savitzky–Golay method (7 points, Spectra Manager, JASCO). For baseline correction, a subtraction of polynomial-fitted baseline was performed. All spectra were normalized with a standard band of 1450 cm^{-1}, which is assigned to the CH_2 deformation mode. The spectra were obtained from the nuclei of 131 neural cells in 5 culture dishes in total. They were derived from 25 fetuses obtained from 2 rats in twice independent experiments.

2.4 Immunostaining and fluorescent observation

Immunostaining was employed in order to identify types of neurons after their Raman spectrum was detected. The dish of neurons was put through the immunostaining procedure immediately after the Raman measurement. We identified the neuron from the Raman spectrum according to the recorded grid number and its shape, and then we determined its type. Information regarding each neuron's type was combined with the data retrieved from the Raman spectrum, which was then transferred into the further analysis.

The cells were washed with PBS(−) twice and then fixed with 100% methanol (Wako) at −20 °C for 10 min. Methanol was removed by immersing the sample in PBS(−) 3 times for 5 min each. The fixed cells were treated with 0.2% Triton X-100 in PBS(−) for 1 min to permeabilize cell membrane, then they were incubated with 10% goat serum in PBS(−) at 37 °C for 1 h. An antibody for microtubule-associated protein 2 (MAP2) was used to visualize the neuron body. The antibody for glutamate decarboxylase 67 (GAD67) was used to identify inhibitory neurons. The sample was incubated overnight at 4 °C with the anti-MAP2 antibody (rabbit polyclonal, 1 : 1000, Millipore) and anti-GAD67 antibody (mouse monoclonal, 1 : 500; Millipore) in 10% of normal goat serum and 0.2% Triton X-100 in PBS(−). It was washed with PBS(−) 3 times for 5 min each,

then combined with the secondary antibodies, Alexa Fluor®546 combined anti-rabbit IgG and Alexa Fluor®488 combined anti-mouse IgG (Molecular Probes®), and incubated at room temperature for one hour. Fluorescent images were captured by a Nikon confocal microscope system A1 (Nikon).

2.5 PLSR-DA calibration model

All chemometrics procedures were performed using the software The Unscrambler X (CAMO). Datasets for excitatory and inhibitory neurons were marked with dependent variables of "−1" or "1" to build the discrimination model with PLSR-DA. Factors to build a reliable model were selected to make the root mean squared error (RMSE) to be small enough. The PLSR-DA model was optimized by selecting effective frequency regions. The discrimination model was validated with a separate test dataset. A training set included 109 spectra collected from 4 culture dishes and a test set had 25 spectra collected from one independent culture dish.

3. Results and discussion

A procedure for the low-density culturing of primary neurons was developed in the present study. It was necessary to visually determine and mark each neuron on the dish in order to measure individual Raman spectra. The type of neuron was subsequently identified using immunostaining. A glial feeder layer was necessary to keep the low-density neural cells in an active condition. The glial cell is able to support and induce normal maturation of neurons. The low-density neurons without the glial feeder layer showed luck or suppression of the axon extension and were destroyed during a long culture term. Raman measurement of the neurons was carried out at 15 days in vitro (DIV). The position and shape of each neuron was recorded carefully during the measurements. The cells in the dish were stained immediately after the Raman measurements in order to determine their types. The amino acid γ-amino-butyric-acid (GABA) is an inhibitory

neurotransmitter and regulates neural activity in both of the central and peripheral nervous systems in adult mammals. GAD67 is one of the essential GABA producing proteins in the inhibitory neuron.[28] The neurons in the cultured dish were stained with anti-MAP2 and anti-GAD67 antibodies.

Fig. 1 depicts a bright field image (a) and a fluorescent image (b) of neurons. The neurons are colored in red, and only the inhibitory one shows green fluorescence. We have observed 131 cells expressing MAP2, which is a marker of neurons, and found only 12 cells stained with GAD67. The other 119 cells were excitatory ones. These results suggested that the primary cultured neurons could be differentiated into excitatory or inhibitory neurons, and the rate of inhibitory neurons was 9.2%. It was reported that the rate of inhibitory neuron is generally several 10% in the cerebral cortex of adult rodents.[29] Fig. 2 shows the average Raman spectra of excitatory (a) and inhibitory (b) neurons, and their difference (c; spectrum (b) – spectrum (a)). The spectral features are similar to one another. The bands at 782 and 828 cm^{-1} were assigned to O–P–O symmetric and asymmetric stretching modes of nucleic acid. Bands at 852 and 1003 cm^{-1} arise from ring breathing modes of tyrosine and phenylalanine. A band at 1093 cm^{-1} seems to be attributed to PO^{2-} stretching mode. Bands at 1126, 1174, 1245, 1450 and 1659 cm^{-1} seems to have a large contribution from C–N stretching, C–H bending, amide III, CH deformation, and amide I modes of protein, respectively.[30,31] A band at 1338 cm^{-1} is assignable to overlapping modes due to adenine, guanine, and C–H deformation mode of protein. In contrast, the difference spectrum has different features then those of these major bands. Although the positive and negative bands in the difference spectrum may be attributed to proline and hydroxyproline, the difference spectrum is too noisy for discrimination of neuron types.

PLSR-DA was used to build a discrimination model for excitatory and inhibitory neurons. The model was evaluated with leave-one-out cross validation for the full region of 760–1800 cm^{-1}. The number of factors that provided a minimum RMSE value was 3,

which suggests that only the first 3 factors have a strong contribution to the discrimination between excitatory and inhibitory neurons. The predictive result of this model is shown in Fig. 3(a). Several inhibitory neurons were misclassified as excitatory neurons. Fig. 3(b) shows the weighted regression coefficients reflecting loadings, as well as the weights of the first 3 factors, which represent important variables for the building model. Some bands in the regression coefficient spectrum were commonly observed in the different spectrum in Fig. 2(c) but overall, the features are rather different. The positive (1060, 1279, 1316 and 1400 cm^{-1}) and negative (821, 955 and 1045 cm^{-1}) bands may be assignable to proline and hydroxyproline. Since some major bands of proline and hydroxyproline were missing in the spectrum, we assumed that it reflected structural changes of material in the cytoplasm. There are likely intermediate filaments that compose the cell cytoskeleton, because it has rich hydroxyproline and proline in its components. Kono et al. suggested that the axons of excitatory neurons grow significantly longer than those of inhibitory neurons in the early stages of development.[32]

Because the regression coefficient had strong noise, the spectral area was carefully restricted and selected to improve the result of cross-validation results. The validation result of optimized discrimination model is shown in Fig. 3(c). The model was rebuilt with following bands and spectral areas: 776, 782, 794–798, 816–840, 847–857, 870, 875, 881–890, 914, 931 971, 979–982, 988–991, 997–999, 1015–1017, 1037–1067, 1182, 1197–1201, 1211–1214, 1246–1274, 1314–1321, 1358, 1365, 1395–1408, 1418–1424, 1434, 1458, 1464–1467, 1483 1492, 1497, 1503–1506, 1540–1587, 1598, 1611–1638 cm^{-1}. After the optimization, the RMSE was reduced to 0.335. The prediction values for the inhibitory neurons were closer to 1 in this model, suggesting that the model was remarkably improved. The optimized discrimination model was then verified using unknown data. We employed 25 spectra obtained from a totally independent culture dish. Fig. 4 shows the training datasets (a) of the optimized PLSR-DA model and validation results (b) of the unknown test datasets. The results showed that the excitatory and

inhibitory neurons were successfully differentiated using the present technique. The result assures that they are different in molecular compositions. In contrast, the averaged prediction values and deviations for the excitatory and inhibitory neurons were −0.66 ± 0.32 and 0.36 ± 0.32. It suggests that the present Raman spectra and the discrimination model include relatively large deviations. It is necessary to reduce noise and to increase numbers of the Raman data for building a more robust and reliable discrimination model.

4. Conclusion

The study demonstrates that Raman spectroscopy with PLSR-DA has a high potential for intact discrimination between excitatory and inhibitory neurons. The discrimination model shows the best results for a model built with only 3 factors and gives good discrimination results for an unknown dataset. This strongly suggests that the model has high applicability in discrimination analysis of neural types. The bands, due to hydroxyproline and proline, are observed in the weighted regression coefficients. This suggests that excitatory and inhibitory neurons have differences in the structures of their intermediate filaments that compose their cytoskeletons.

References

1. R. D. Fields and B. Stevens-Graham, *Science*, 2002, **298**, 556-562.
2. C. G. Dotti, C. A. Sullivan and G. A. Banker, *Journal of Neuroscience*, 1988, **8**, 1454-1468.
3. W. Yu and P. W. Baas, *Journal of Neuroscience*, 1994, **14**, 2818-2829.
4. C. H. Davies and G. L. Collingridge, *Journal of Physiology*, 1996, **496**, 451-470.
5. C. E. Ribak, J. E. Vaughn, K. Saito, R. Barber and E. Roberts, *Brain Research*, 1976, **116**, 287-298.
6. A. Kiyohara, T. Taguchi and S. N. Kudoh, *IEEJ Transactions on Electronics, Information and Systems*, 2009, **129**, 1815-1821.
7. D. Ito, H. Tamate, M. Nagayama, T. Uchida, S. N. Kudoh and K. Gohara, *Neuroscience*, 2010, **171**, 50-61.
8. K. Hashimoto, S. Kudoh and H. Sato, *Analyst*, 2015, **140**, 2344-2349.
9. N. Tamamaki, Y. Yanagawa, R. Tomioka, J. Miyazaki, K. Obata and T. Kaneko, *Journal of Comparative. Neurology*, 2003, **467**, 60-79.
10. D. Evanko, *Nature Methods*, 2006, **3**, 76.
11. J. D. Pédelacq, S. Cabantous, T. Tran, T. C. Terwilliger and G. S. Waldo, *Natature Biotechnology*, 2006, **24**, 79-88.
12. K. Hayashi, R. Kawai-Hirai, A. Harada and K. Takata, *Journal of Cell Science*, 2003, **116**, 4419-4428.
13. K. Hamada, K. Fujita, N. I. Smith, M. Kobayashi, Y. Inouye and S. Kawata, *Journal of Biomedical Optics*, 2008, **13**, 044027.
14. I. Notingher, S. Verrier, H. Romanska, A. E. Bishop, J. M. Polak and L. L. Hench, *Spectroscopy*, 2002, **16**, 43-51.
15. A. Ghita, F. Pascut, M. Mather, V. Sottile and I. Notingher, *Analytical Chemistry*, 2012, **84**, 3155-3162.
16. H. J. Butler, L. Ashton, B. Bird, G. Cinque, K. Curtis, J. Dorney, K. Esmonde-

White, N. J. Fullwood, B. Gardner, P. L. Martin-Hirsch, M. J. Walsh, M. R. McAinsh, N. Stone, F. L. Martin, *Nature Protocols*, 2016, **11**(4), 664-687

17. A. Taketani, R. Hariyani, M. Ishigaki, B. Andriana and H. Sato, *Analyst*, 2013, **138**, 4183-4190.
18. H. Yao, Z. Tao, M. Ai, L. Peng, G. Wang, B. He and Y. Li, *Vibrational Spectroscopy*, 2009, **50**, 193-197.
19. S. Morita, S. Takanezawa, M. Hiroshima, T. Mitsui, Y. Ozaki and Y. Sako, *Biophys. J.*, 2014, **107**, 2221-2229.
20. S. Duraipandian, W. Zheng, J. Ng, J. J. H. Low and A. Ilancheran, *Anal. Chem.*, 2012, **84**, 5913-5919.
21. G. R. Lloyd, L. E. Orr, J. Christie-Brown, K. McCarthy, S. Rose, M. Thomas and N. Stone, *Analyst*,2013, **138**, 3900-3908.
22. M. Barker and W. Rayens, *Journal of chemometrics*, 2003, **17**, 166-173.
23. C. Mello, D. Ribeiro, F. Novaes and R. J. Poppi, *Anal. Bioanal. Chem.*, 2005, **383**, 701-706.
24. P. Heraud, J. Beardall, D. McNaughton and B. R. Wood, *FEMS Microbiol. Lett.*, 2007, **275**, 24-30.
25. M. S. Bergholt, W. Zheng, K. Lin, K. Y. Ho, M. Teh, K. G. Yeoh, J. B. Y. So and Z. Huang, *Analyst*, 2010, **135**, 3162-3168.
26. A. Taketani, B. B. Andriana, H. Matsuyoshi and H. Sato, *Analyst*, 2017, **142**, 3680-3688.
27. H. Sato, S. Wada and H. Tashiro, *Applied Spectroscopy*, 2002, **56**, 1303-1307.
28. M. Esclapez, N. J. Tillakaratne, D. L. Kaufman, A. J. Tobin and C. R. Houser, *J. Neurosci.*, 1994, **14**, 1834-1855.
29. K. Kameyama, K. Sohya, T. Ebina, A. Fukuda, Y. Yanagawa and T. Tsumoto, *J. Neurosci.*, 2010, **30**, 1551-1559.

30. Y. Oshima, H. Shinzawa, T. Takenaka, C. Furihata and H. Sato, *Journal of Biomedical Optics*, 2010, **15**, 017009.

31. Z. Movasaghi, S. Rehman and I. Rehman, *Applied Spectroscopy Reviews*, 2007, **42**, 493-541.

32. S. Kono, H. Yamamoto, T. Kushida, A. Hirano-Iwata, M. Niwano and T. Tanii, *PLoS One*, 2016, **11**, e0160987.

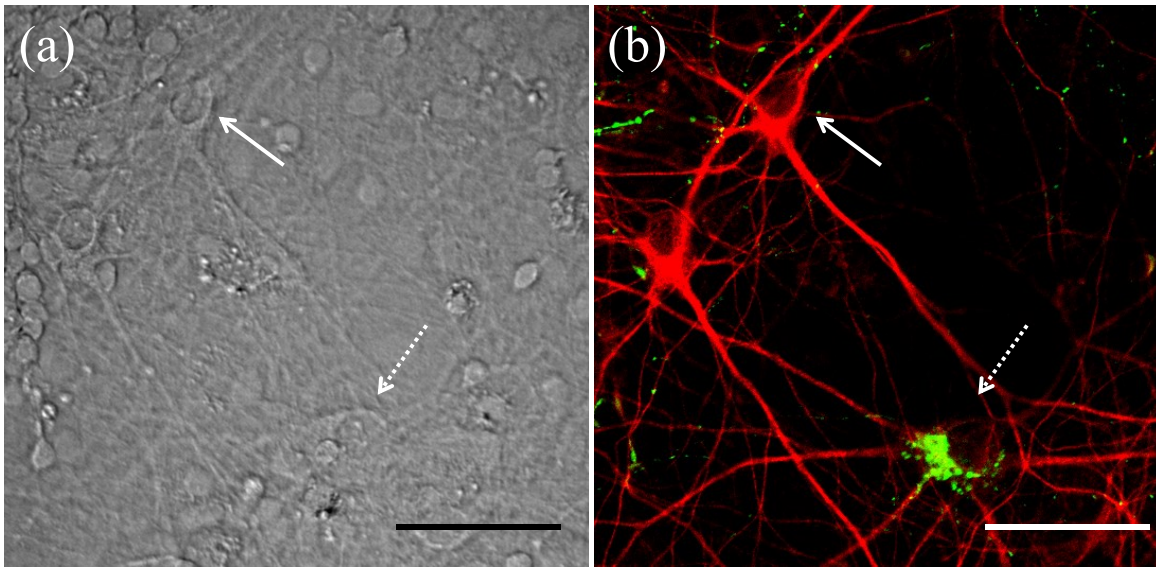

Figure 1

Representative photomicrographs of neurons in the network built on the culture dish at 15 days in vitro (DIV). (a) An image of the intact neurons observed under the Raman microscope. (b) A fluorescent image of neurons immunostained with MAP2 (red) and GAD67 (green). The umages show the same site. Solid arrows and dashed arrows point to the excitatory and inhibiory neurons, respectively. The scale bars are 50 μm.

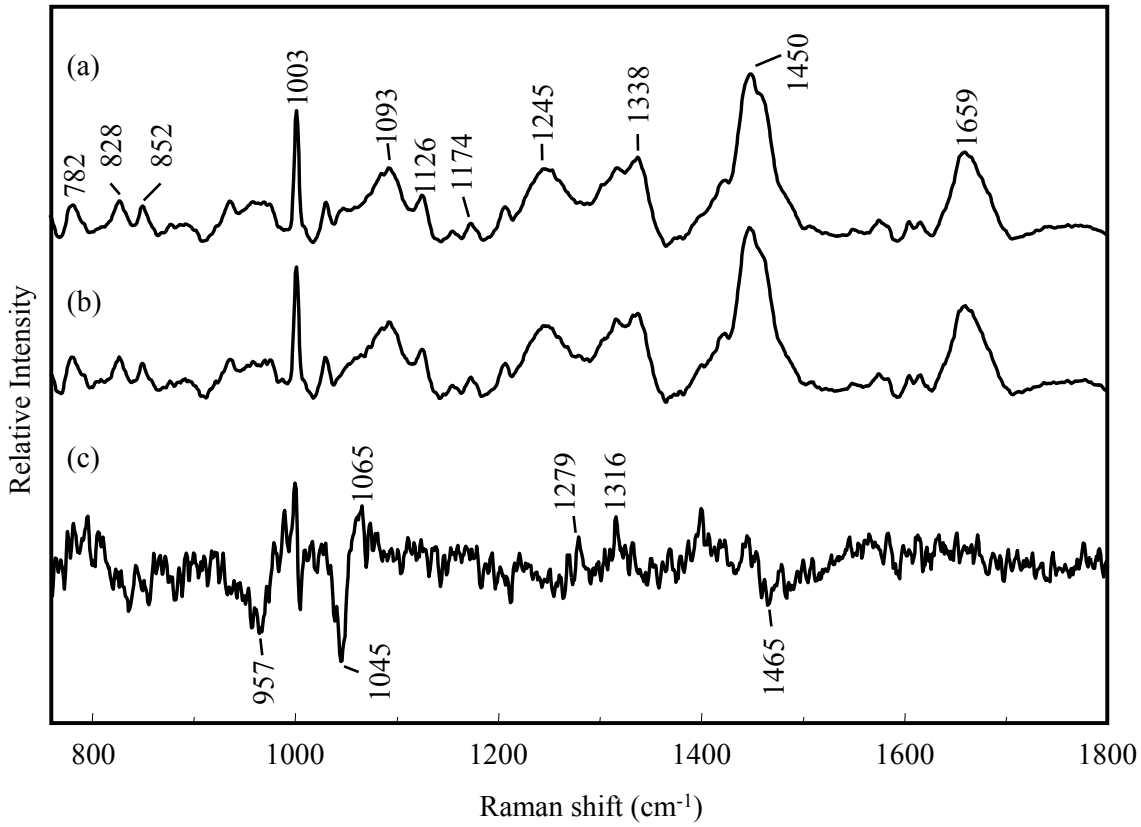

Figure 2

Raman spectra of the neurons on the cultured dish at 15 DIV. (a) Average spectrum of excitatory neurons (n = 119). (b) Average spectrum of inhibitory neurons (n = 12). (c) The spectrum made by subtracting (b) from (a).

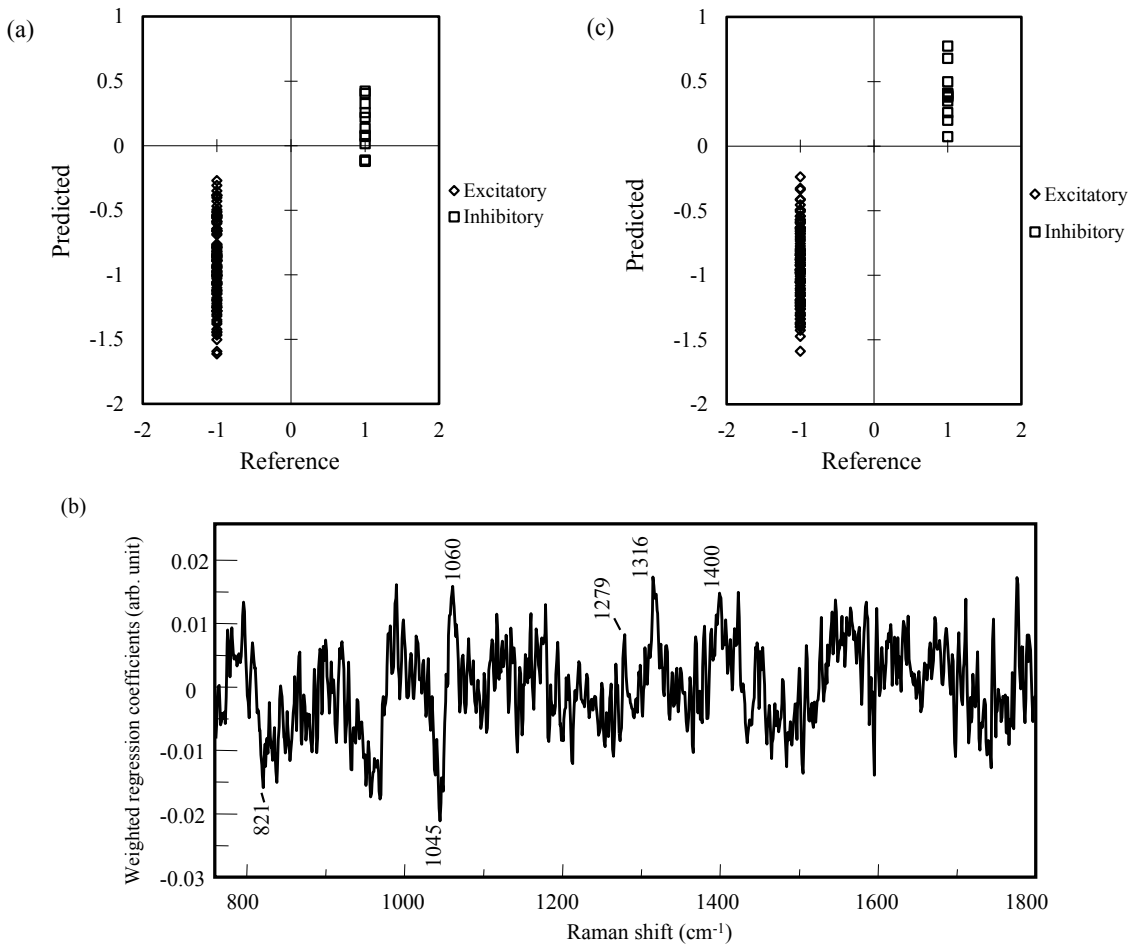

Figure 3

Discrimination plots (predictive versus reference) of the leave-one-out cross validation results for the PLSR-DA models. (a) The result for the PLSR-DA model built with a full spectral region (760—1800 cm^{-1}). (b) Weighted regression coefficients of factors for the PLSR-DA model built with a full spectral region. (c) The result for the optimized PLSR-DA model.

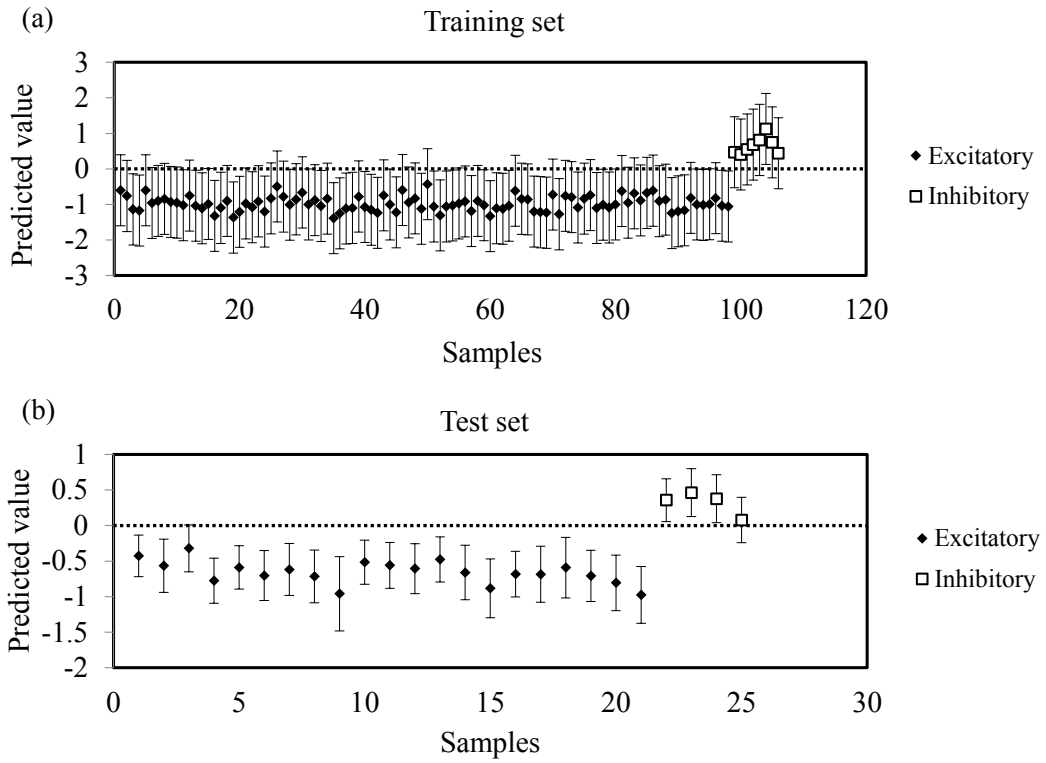

Figure 4

Validation results of the optimized PLSR-DA model. (a) The discrimination plot for the training dataset. (b) The discrimination plot for the independent test dataset.

Chapter 3

Raman spectroscopic analysis of the effect of chemical treatment on a developing neuron

Abstract

Molecular changes in a live neural cell caused by an endocrine disruptor, bisphenol A (BPA), were studied using Raman spectroscopy. BPA is a harmful chemical that disrupts the development of brain. An in vitro electrophysiological study suggested that BPA inhibits the signaling activity of neural cells. A Raman analysis of the molecular composition of a growing neural cell suggested that it has several maturation stages correlating with its function. In the present study, the origin of the inhibition of its signaling activity was studied by Raman spectroscopy. As the molecular composition changes with the growth of the neural cell, there are 2 possible mechanisms behind the observed functional inhibition; degeneration in the maturation stage and disorder in the cellular constancy. Principal component analysis (PCA) of the Raman spectra obtained from the control and BPA exposed cells suggested that molecular changes occur in the BPA exposed cells. These changes did not seem to affect maturation of the neural cell. A comparative study between control and BPA exposed cells suggested that BPA causes a disorder in the cellular constancy, resulting in molecular compositional changes.

1. Introduction

An endocrine disruptors is a chemical with a molecular structure similar to that of a natural hormone and which interferes endocrine system.[1] Some disruptors cause irregular growth of the brain, especially during the development of the brain. The young immature brain is highly sensitive even to low concentrations of endocrine disruptors.[2] Exposure to endocrine disruptors increases the risk of nerve disease. Harley et al. reported that exposure to the organophosphorus pesticide increased the risk of development of attention-deficit hyperactivity disorder (ADHD) among children.[3] Bisphenol A (BPA) is an endocrine disruptor that is abundantly included in plastics and epoxy resins used in ordinary products.[4] Ishido et al. reported that the mouse pups developed hyperactivity disorder when maternally exposed to BPA via oral intake.[5] The gene expression levels of the dopamine D4 receptor and dopamine transporter decreased remarkably in the brain of rat pups born from a dam exposed to BPA. Although it has been suggested that BPA may have an effect on neural cells during the development and/or maturation of the rat pup, the associated mechanisms have not been revealed yet. The effect of early BPA exposure on neural cells has not been studied in detail. Ito et al. studied the electric signaling in cultured neural cells exposed to BPA.[6] They suggested that BPA inhibits the intrinsic signaling of cells at any stage of maturation but the time to recovery of their function is shorter for mature cells. This suggests that immature neural cells have a higher sensitivity to BPA.

The purpose of the present study is to investigate the effect of BPA on neural cells. Raman analysis was employed to reveal if BPA inhibits or accelerates the growth of neural cells. In my previous study (Chapter 1), I studied the molecular compositional changes in neural cells during normal maturation in vitro by Raman analysis. If the BPA merely modifies the maturation stage of the neural cell, the Raman spectra of the BPA exposed cells are categorized into any stage of the analytical model. If it does not, their spectra are categorized into a new data group.

2. Materials and methods

2.1 Sample preparation

A dissociated culture of rat hippocampal neurons was employed for the experiment. The procedure for primary culturing was the same as that used in our previous report.[7] Briefly, dissection of the hippocampus was performed in a Wistar rat fetus on embryonic day 18. After dissection, the hippocampus was dissociated into single cells via treatment with 0.125% trypsin‐EDTA in a phosphate buffered saline without Ca^{2+} and Mg^{2+}. The suspension was diluted with cell culture medium. The culture medium consisted of Neurobasal A medium supplemented with a B27 supplement and 100 unit/ml penicillin-streptomycin. Neural cells were seeded onto quartz glass bottom dishes at a density of 250 cells/mm^2. The cells were cultured at 37 degrees Celsius and 5% CO_2 in an incubator. Medium change was performed every 2 days.

BPA was dissolved in ethanol and a 20 μl solution was added into the culture medium. The BPA exposed sample were prepared at a final concentration of 10 and 100 μM. The sample treated with 20 μl ethanol was used as the control. BPA treatment was performed 3 days in vitro (DIV) for 24 hours. After the treatment, the medium was replaced with fresh culture medium without BPA.

2.2 Micro-Raman spectroscopy

The Raman spectra were collected from the nuclei of the neurons at 4, 10 and 15 DIV. The apparatus and measurement condition was the same as that described in chapters 1 and 2. Briefly, a confocal Raman microscope system (Nanofinder30, Tokyo instruments) was equipped with a 60× water immersion objective lens (N.A. 1.1, LUMFLN, Olympus), CO_2 chamber (Tokai hit), and an XY motor driven stage (Chuo precision industrial). The detection part consists of a spectrometer equipped with a 600 lines per mm grating (blazed at 750 nm) and a water-cooled CCD (driven at −80 °C; DU420-BRDD; Andor Technology). An excitation light at 785 nm was provided from a

continuous-wave background-less electrically tuned Ti:Sapphire laser (CW-BL-ETL) in order to avoid contamination of spontaneous fluorescent from the laser-active medium.[8] The laser was focused on the nucleus of the neuron with 30 mW laser power. Acquiring the Raman spectrum took 90 seconds.

2.3 Data analysis

The background spectra of the quartz substrate and cell culture medium were subtracted from the raw spectra. Further background correction was carried out by subtracting the 11th-order polynomial-fitted background to remove the baseline undulation attributed to the autofluorescence of proteins. The spectra were normalized with a standard band at 1450 cm^{-1} corresponding to the CH_2 deformation mode.

The Raman spectra were analyzed with The Unscrambler multivariate analysis software (Camo). In this study, principal component analysis (PCA) was performed to investigate the effect of exposure to BPA on the molecular compositional changes in the neural cell.

3. Results and discussion

The Raman spectra of the neural cells are compared in Fig. 1. The spectra of the control cells cultured for 4 (a), 10 (b) and 15 DIV (c) were similar to those of the cells exposed to BPA also cultured for DIV 4 ((d) 10 μM and (g) 100 μM), 10 DIV ((e) 10 μM and (h) 100 μM) and 15 DIV ((f) 10 μM and (i) 100 μM). The cells exposed to BPA for 1 week also showed similar spectral features. The bands at 1003, 1256 and 1660 cm^{-1} were assigned to the ring breadth of phenylalanine, amide Ⅲ and amide Ⅰ modes of protein, respectively.[9, 10] The bands at 785 cm^{-1} were assigned to the O-P-O stretching mode of nucleic acids.

To detect the spectral changes due to BPA, a PCA prediction model was built only with the datasets of the control cells. Then, the datasets of the BPA exposed cells

were plotted on the prediction model. The test datasets of the BPA exposed cells obtained at 4 (a), 10 (b), and 15 (c) DIV were plotted on the prediction model score plot in Fig. 2. The datasets of the control cells were categorized into 3 groups in the score plot of PCs 2 and 3 of the prediction model. Although their dispersion overlapped, they shifted from the upper right to the lower left along with the days of culturing. The overlap between the datasets at 4 DIV and 10 DIV was small but that between the datasets at 10 DIV and 15 DIV was much larger. In my previous work, PCA analysis of the in vitro cultured neural cells suggested a stepwise molecular change with cell growth. The present results corroborate with these previous findings. The control dataset of the DIV 4 cells was divided into 2 groups in the PC 3 axis. The datasets included spectra obtained in several repeated experiments in which neural cells were collected from different pregnant rats. These results indicated 2 possibilities: one is that neural cells are extremely sensitive to the cultivation conditions; the other is that the spectral difference during the 4 to 15 DIVs is as small as the individual difference between the rats. The loading plot of PCs 1, 2 and 3 are depicted in Fig. 3. They included high noise, indicating that the difference among the spectra is as small as the noise level. The plotted datasets of the BPA exposed cells showed a relatively smaller dispersion than that with the control datasets. The dataset of 4 DIV showed good overlapping with that of the control dataset at 4 DIV. Those at 10 DIV and at 15 DIV show similar overlapping. The present prediction model built with the control datasets represented in vitro cell maturation from 4 to 15 DIVs. The results in Fig. 2 suggested that BPA does not result in neural degeneration.

To detect the effect of BPA on neural cells, the datasets of the cells without (control) and with BPA exposure were compared at the same DIVs. Fig. 4 shows the PCA score plots of the datasets at 4 DIV (a; PCs 1 and 2), 10 DIV (b; PCs 1 and 2) and 15 DIV (c; PCs 2 and 3). Here, the components that showed the largest spreading between the datasets of the control and exposed cells were used for the score plots. The BPA exposed cells had a large dispersion in the PC 2 direction in all the score plots. For the datasets at

4 DIV, the cells exposed to 10 μM BPA showed the largest divergence from the control ones but those exposed to 100 μM BPA overlap well over the control ones. Similar results were seen on 15 DIV. In contrast, the score plot of the 10 DIV showed that the control dataset was isolated from data of the BPA exposed cells and the dataset of the cells exposed to 100 μM BPA showed a larger separation than that of the 10 μM BPA from the control dataset. Some data points showed 2 divided data groups within one dataset because the dataset included data obtained from 2 repeated experiments. These phenomena highlight the difficulty of controlling neural cells in vitro.

Loading plots of the PCs used to depict the score plots in Fig. 4 are shown in Fig. 5. The loading plots of PCs for the datasets of the 4 DIV showed a narrower spectral region than those of 10 DIV and 15 DIV, because the region from 1620 to 1800 cm^{-1} was excluded from the analysis. The datasets of the 4 DIV showed the contribution of the medium that had to be removed in the background subtraction procedure. The PC1 in the PCA of the 15 DIV datasets had a broad band near 1640 cm^{-1} that was assignable to water.[11, 12] The PC1 was excluded from further analysis because PC1 did not contribute significantly to the separation of the control and BPA exposed data groups. The band due to water is often observed in PCA results when the spectral subtraction procedure is not sufficiently effective. The loading plot of the 4 DIV had weak negative bands at 1100 and 1491 cm^{-1}. It was, however, difficult to identify the material because the loading plot had a lot of noise. The loading plots of PC2 and PC3 of the datasets of the 10 DIV and 15 DIV also had a lot of noise to estimate the molecules to differentiate the BPA exposed cells from the control ones.

In the PCA analyses, the datasets of the control and BPA exposed cells were integrated ones obtained from two independent experiments. Although the loading plots did not identify the components modified by BPA exposure, the categorized datasets in the score plots were convincing because data obtained from 2 independent experiments showed a similar behavior. For example, the acore of the control dataset was significantly

lower than that of the BPA exposed detaset, which is obvious when their scores in Fig. 4 (b) were compared only in the PC2 axis. The present result demonstrates that Raman analysis is able to detect the effect of endocrine disruptors on neural cells. BPA affects neural cells but it does not interfere with maturation, but disrupts cellular function directly. The present results corroborate those obtained using electrophysiological techniques by Ito et al. Had BPA affected the maturation stage, the more mature cells would have required more time to recover their normal function. However, this was not the case.

4. Conclusion

The present study shows that BPA causes molecular compositional changes in live neural cells. Raman spectroscopy results suggest that the molecular changes may be attributable to direct disorder in the cellular component but not to inhibition or acceleration of maturation.

References

1. H. Gelbke, M. Kayser and A. Poole, *Toxicology*, 2004, **205**, 17-25.
2. N. MacLusky, T. Hajszan and C. Leranth, *Environmental Health Perspectives*, 2005, **113**, 675-679.
3. K. Harley, R. Gunier, K. Kogut, C. Johnson, A. Bradman, A. Calafat and B. Eskenazi, *Environmental Research*, 2013, **126**, 43-50.
4. K. Suzuki, K. Ishikawa, K. Sugiyama and H. Furuta, *Journal of Dental Research*, 2000, **79**, 191-191.
5. M. Ishido, Y. Masuo, M. Kunimoto, S. Oka and M. Morita, *Journal of Neuroscience Research*, 2004, **76**, 423-433.
6. 伊東嗣功, 博士論文, 関西学院大学, 2015.
7. K. Hashimoto, S. Kudoh and H. Sato, *Analyst*, 2015, **140**, 2344-2349.
8. H. Sato, S. Wada and H. Tashiro, *Applied Spectroscopy*, 2002, **56**, 1303-1307.
9. Z. Movasaghi, S. Rehman and I. Rehman, *Applied Spectroscopy Reviews*, 2007, **42**, 493-541.
10. I. Notingher, C. Green, C. Dyer, E. Perkins, N. Hopkins, C. Lindsay and L. Hench, *Journal of the Royal Society Interface*, 2004, **1**, 79-90.
11. W. Kowalchyk, P. Walker and M. Morris, *Applied Spectroscopy*, 1995, **49**, 1183-1188.
12. Y. Oshima, H. Shinzawa, T. Takenaka, C. Furihata and H. Sato, *Journal of Biomedical Optics*, 2010, **15**.

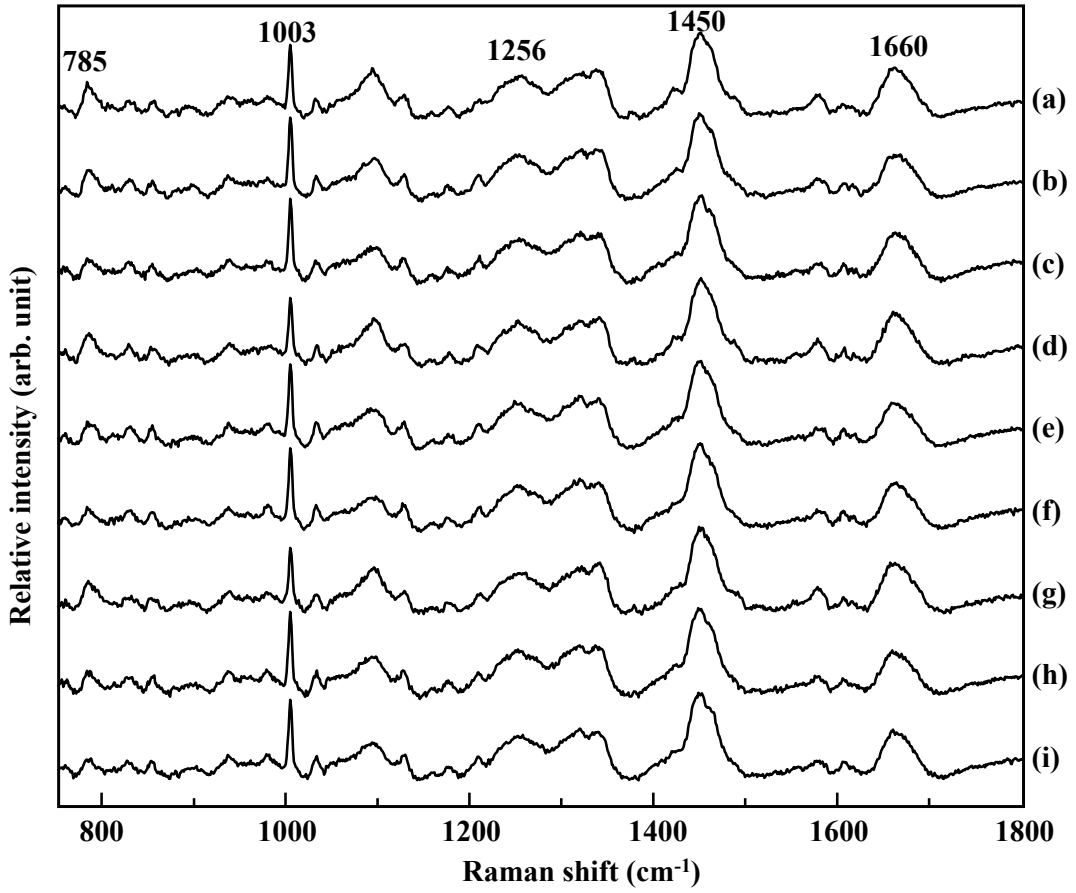

Figure 1

Averaged Raman spectra of the nuclei of the live neurons. The spectra (a) – (c) are those treated without BPA measured at 4, 10 and 15 DIV. The spectra (d) – (f) are those treated with 10 μM BPA measured at 4, 10 and 15 DIV. The spectra (g) – (i) are those treated with 100 μM BPA measured at 4, 10 and 15 DIV, respectively.

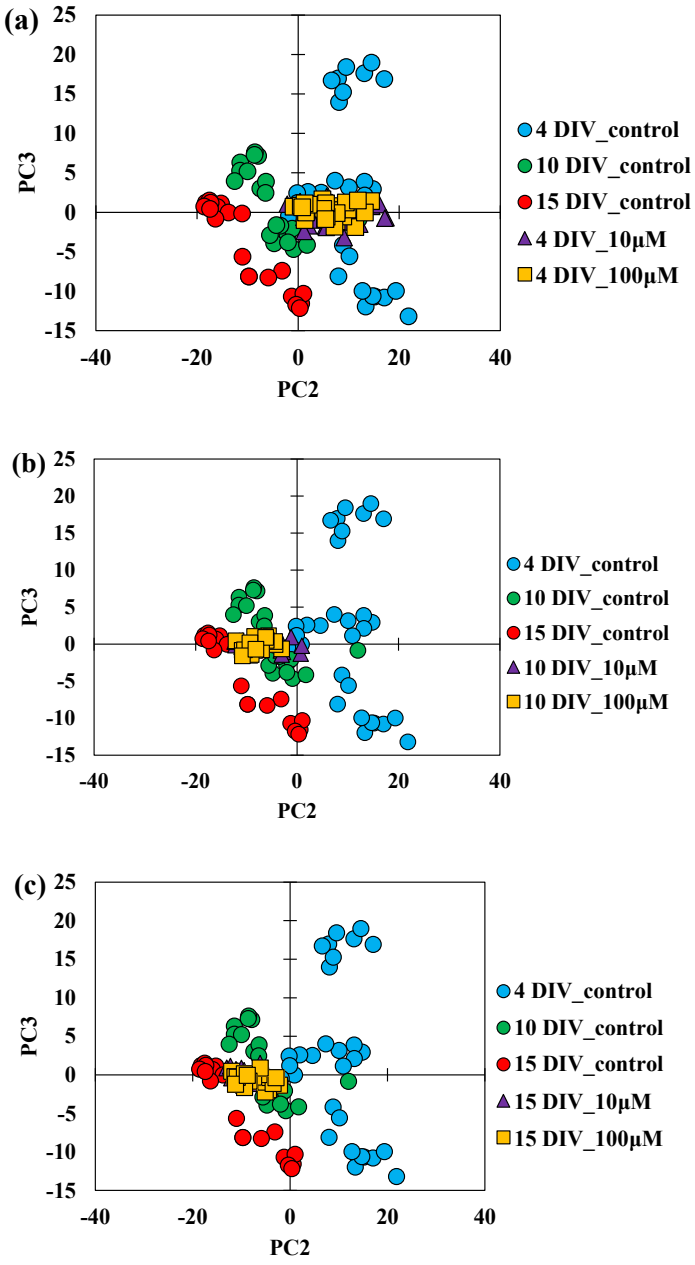

Figure 2

The test datasets of the BPA exposed neurons measured at 4 (a), 10 (b) and 15 DIV (c) plotted on the PCA analytical model built with the control datasets measured at 4, 10 and 15 DIV.

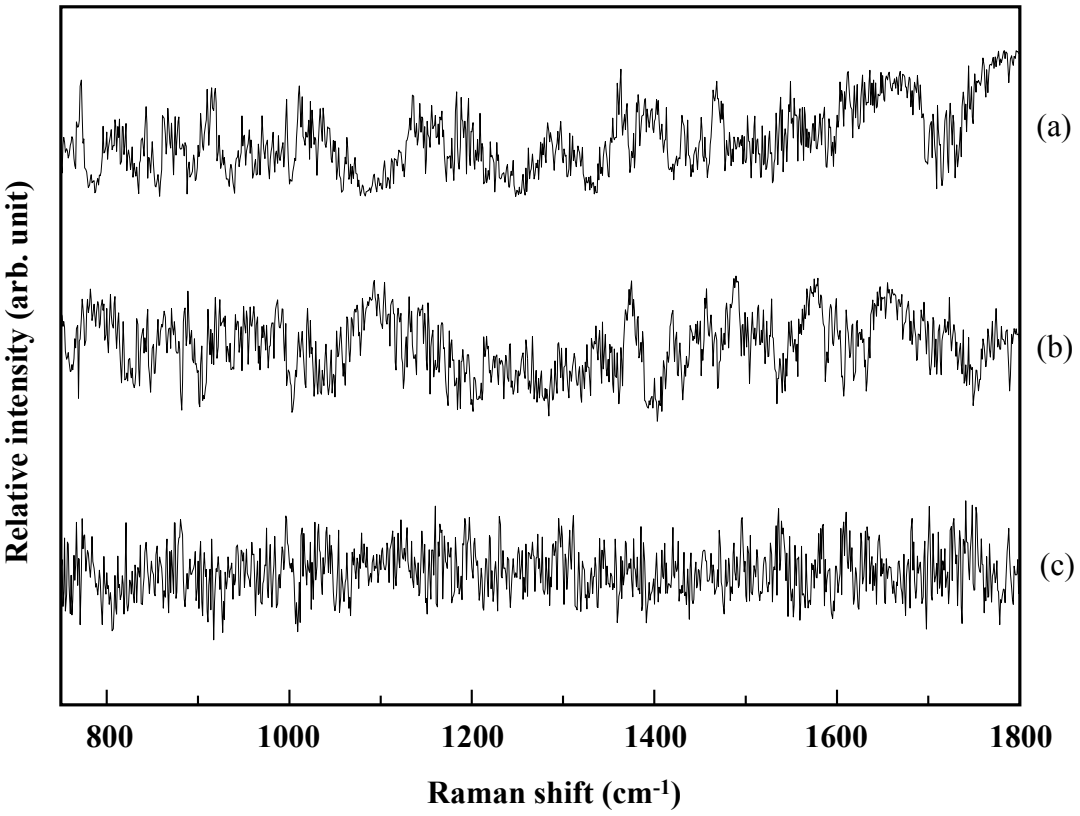

Figure 3

Loading plots of PCs 1 (a), 2 (b) and 3 (c) of the analytical model built with the control datasets.

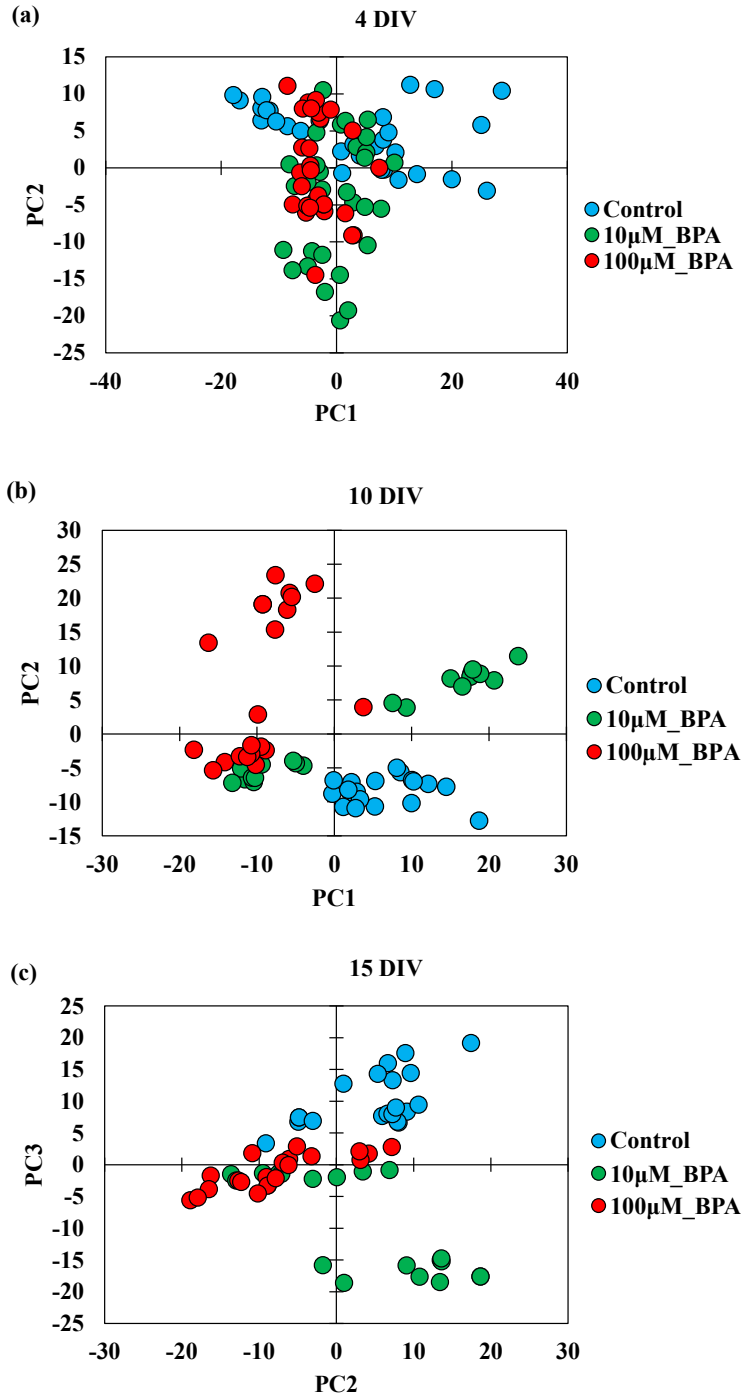

Figure 4

PCA score plots built with the datasets of the control, the neuron exposed to 10 μM, and 100 μM of BPA. The plots are those of the datasets measured at 4 (a), 10 (b), and 15 DIV (c).

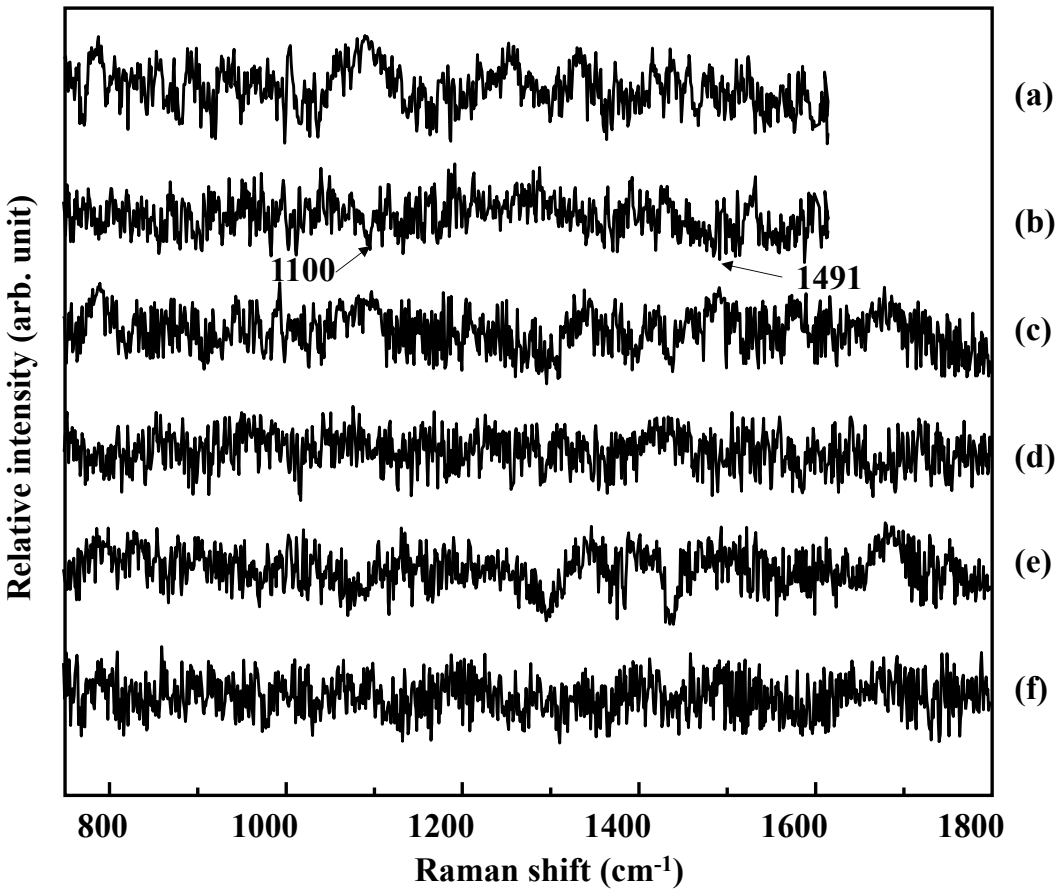

Figure 5

Loading plots of the PCs used in the PCA score plots in Fig. 4. The loading plots (a) and (b) the PCs 1 and 2 of the 4 DIV datasets (Fig. 4(a)). The wavenumber region from 1620 to 1800 cm^{-1} was excluded to exclude the band due to the cell culture media. The PCs 1 (c) and 2 (d) of the 10 DIV datasets (Fig. 4(b)). The PCs 2 (e) and 3 (f) of the 15 DIV datasets (Fig. 4(c)).

General conclusion

The present study investigated changes in the molecular composition of live growing neurons as they are related with functional development. Chapter 1 demonstrates the potential of Raman spectroscopy in the study of molecular compositional changes of intact live neurons during neural network formation in vitro. Although a differentiated neuron arrests its cell cycle, the analysis shows that its molecular composition alters with functional development. The PCA analysis results of the Raman spectra suggests that a neuron has several characteristic stages during growth correlating with its functional development. The PCA model built for a normal neuron in vitro is a good standard for comparing neurons exposed to various chemical materials that are able to affect cell growth. Chapter 2 demonstrates that Raman spectroscopy is capable of discriminating excitatory and inhibitory neurons in a totally non-invasive manner. The validation study using an independent test dataset revealed the reliability of the present analytical model. Although the Raman spectra of excitatory and inhibitory neurons are quite similar, the PLSR-DA technique is effective in extracting differences that are not detected even with PCA. The effect of BPA on a neural cell was successfully detected in chapter 3. The results suggest that the effect of BPA is not to accelerate or decelerate cellular growth. However, exposure to BPA results in dysregulation of cellular growth.

Acknowledgement

For the accopmlishment of this thesis, I have received much help, guidance and encouragement from many people. I'm extreamly grateful to Prof. Hidetoshi Sato, my supervisor, for his sincere guidance, discussion and encouragement. I'd like to express deeply appriciation for Prof. Suguru N. Kudoh for giving the opportunity to study the method of dissociated culture and helpful discussion for this study. I'd like to thank Prof. Susumu Imaoka and Prof. Yohei Hirai for their sincere and critical comments on this study. I am grateful to Dr. Hiroko Matsuyoshi and Dr. Bibin Bintang Andriana for helpful comments in chapter 2. I am also grateful to all members of Sato laboratory.

Finally, I really appreciate to my family for their wholehearted support and dedicate this thesis as a compilation of the education they have given.

List of publications

Original papers:

1. Kosuke Hashimoto, Bibin B. Andriana, Hiroko Matsuyoshi, Hidetoshi Sato, “Discrimination analysis of excitatory and inhibitory neurons by Raman spectroscopy” *Analyst*, Royal society of chemistry, **143**, pp 2889-2894, 2018
2. 橋本剛佑，松吉ひろ子，佐藤英俊，「ラマン分光法を用いた神経細胞成熟過程の観察」，*生物物理*，57 (4), pp 208-211, 2017.
3. Mika Ishigaki, Kosuke Hashimoto, Hidetoshi Sato, Yukihiro Ozaki, “Non-destructive monitoring of mouse embryo development and its qualitative evaluation at the molecular level using Raman spectroscopy”, *Scientific Reports*, **7**, 43942, 2017
4. Kosuke Hashimoto, Suguru N. Kudoh, Hidetoshi Sato, “Analysis of the developing neural system using an in vitro model by Raman spectroscopy”, *Analyst*, Royal society of chemistry, **140**, pp 2344 – 2349, 2015.
5. Hideyuki Shinzawa, Kosuke Hashimoto, Hidetoshi Sato, Wataru Kanematsu, Isao Noda, Multiple-perturbation two-dimensional (2D) correlation analysis for spectroscopic imaging data, *Journal of molecular structure*, **1064**, pp 176-182, 2014.
6. 橋本剛佑，工藤卓，佐藤英俊，“顕微ラマン分光法による神経細胞成熟のモニタリング分析”，レーザー研究，レーザー学会，**40**，pp 280-284，2012.

Proceedings:

1. Kosuke Hashimoto, Suguru N. Kudoh, and Hidetoshi Sato. "Raman study of analysis for the states of maturation of neural cell", *Proceedings of SPIE*, SPIE, **8939**, 39, 2014.
2. 橋本剛佑，工藤卓，佐藤英俊，「ラマン分光法を用いた神経細胞の機能と分子組成変化の相関解析」，*レーザー学会第 437 回研究会報告：ニューロフォトニクス*，No.RTM-12-66, pp 25-29，2012.